

Glacial lake outburst flood hazard under current and future conditions: worst-case scenarios in a transboundary Himalayan basin

Simon K. Allen^{1,2}, Ashim Sattar¹, Owen King³, Guoqing Zhang^{4,5}, Atanu Bhattacharya^{3,6}, Tandong Yao^{4,5}, Tobias Bolch³

¹Department of Geography, University of Zurich, Zurich, CH-8057, Switzerland

²Institute for Environmental Science, University of Geneva, CH-1205, Geneva

³School of Geography and Sustainable Development, University of St Andrews, St Andrews, KY16 9AL, UK

10 ⁴Key Laboratory of Tibetan Environmental Changes and Land Surface Processes, Institute of Tibetan Plateau Research, Chinese Academy of Sciences (CAS), Beijing, China

⁵CAS Center for Excellence in Tibetan Plateau Earth Sciences, Beijing, China

⁶Department of Remote Sensing & GIS, JIS University, Kolkata 700109, India

Correspondence to: Simon K. Allen (skallenz@gmail.com)

15 **Abstract**

Glacial lake outburst floods (GLOFs) are a major concern throughout High Mountain Asia, where societal impacts can extend far downstream. This is particularly true for transboundary Himalayan basins, where risks are expected to further increase as new lakes develop. Given the need for anticipatory approaches to disaster risk reduction, this study aims to demonstrate how the threat from a future lake can be feasibly assessed along-side that of worst-case scenarios from current lakes, and how this information is relevant for disaster risk management. We have focused on two previously identified dangerous lakes (Galongco and Jialongco), comparing the timing and magnitude of simulated worst-case outburst events from these lakes both in the Tibetan town of Nyalam and downstream at the border with Nepal. In addition, a future scenario has been assessed, whereby an avalanche-triggered GLOF was simulated for a potential large new lake forming upstream of Nyalam. Results show that large ($> 20 \text{ mil m}^3$) rock and/or ice avalanches could generate GLOF discharges at the border with Nepal that are more than 15 times larger than what have been observed previously, or anticipated based on more gradual breach simulations. For all assessed lakes, warning times in Nyalam would be only 5 – 11 minutes, and 30 minutes at the border. Recent remedial measures undertaken to lower the water level at Jialongco would have little influence on downstream impacts resulting from a very large magnitude GLOF, particularly in Nyalam where there has been significant development of infrastructure directly within the high-intensity flood zone. Based on these findings, a comprehensive approach to disaster risk management is called for, combining early warning systems with effective land use zoning and programs to build local response capacities. Such approaches would address the current drivers of GLOF risk in the basin, while remaining robust in the face of worst-case, catastrophic outburst events that become more likely under a warming climate.

Keywords

35 Glacial lake outburst flood, process chain, hazard, risk, future, Himalaya

1 Introduction

Widespread retreat of glaciers has accelerated over recent decades in the Himalaya as in most other mountain regions worldwide as a consequence of global warming ((Bolch *et al.*, 2019; King *et al.*, 2019; Maurer *et al.*, 2019; Zemp *et al.*, 2019). A main consequence has been the rapid expansion and new formation of glacial lakes (Gardelle *et al.*, 2011; Nie *et al.*, 2017; Shugar *et al.*, 2020), which has large implications for both water resources and hazards (Haeberli *et al.*, 2016a). When water is suddenly and catastrophically released, Glacial Lake Outburst Floods (GLOFs) can devastate lives and livelihoods up to hundreds of kilometres downstream (Carrivick and Tweed, 2016; Lliboutry *et al.*, 1977). This threat is most apparent in the Himalaya, where glacial lakes have been increasing rapidly in both size and number (Zhang *et al.*, 2015; Wang *et al.* 2020; Chen *et al.* 2021), and where a frequency of 1.3 GLOFs per year has been recorded since the 1980s (Veh *et al.*, 2019). The fact that GLOFs can extend across national boundaries exacerbates the challenges for early warning or other risk reduction strategies, particularly in politically sensitive regions (Allen *et al.*, 2019; Khanal *et al.*, 2015a).

Lakes can develop either underneath (subglacial), at the side, in front (proglacial), within (englacial), or on the surface of a glacier (supraglacial), with the dam being composed of ice, moraine, or bedrock. In Asia, most scientific attention has focussed upon the hazard associated with the catastrophic failure of moraine-dammed lakes, and particularly those trapped behind proglacial moraines (e.g., Fujita *et al.*, 2013; Westoby *et al.*, 2014; Worni *et al.*, 2012). Such lakes can be very large, with volumes larger than 100 million m^3 (Zheng *et al.* 2021b), and depths exceeding 200 m (Cook and Quincey, 2015), and are susceptible to a range of failure mechanisms owing to the low material strength of the dam structure (Clague and Evans, 2000; Korup and Tweed, 2007). In Asia, as elsewhere in the world, displacement waves generated from large impacts of ice or rock

55 have contributed to the majority of moraine dam failures, occurring predominantly over the warm summer months (Emmer and Cochachin, 2013; Liu *et al.*, 2013; Richardson and Reynolds, 2000). At least 17 GLOF disasters (causing loss of life or infrastructure) have been documented in Tibet since 1935, mostly originating in the central-eastern section of the Himalaya (Nie *et al.*, 2018). Coupled with rapidly increasing population and infrastructural development in the region, an urgent need for authorities to take action and implement timely risk reduction measures has been acknowledged (Wang and Zhou, 2017),
60 considering the best available knowledge on existing threats (e.g., Allen *et al.*, 2019; Wang *et al.*, 2015a, 2018), but also with a view to the future (Furian *et al.*, 2021; Zheng *et al.*, 2021a).

Despite no clear trend observed in GLOF activity over recent decades in the Himalaya (Veh *et al.*, 2019), the ongoing expansion of lakes towards steep and potentially destabilised mountain flanks is expected to lead to new challenges in the
65 future with implications for hazards and risk (Haeberli *et al.*, 2016b). Based on approaches to model the possible future expansion and development of new lakes (Linsbauer *et al.*, 2016) several studies have aimed to quantify the possible implications for GLOF frequency and/or magnitude for different regions (Allen *et al.*, 2016; Emmer *et al.*, 2020; Magnin *et al.*, 2020). For example, in the Indian Himalayan state of Himachal Pradesh, Allen *et al.* (2016) demonstrated a 7-fold increase in the probability of GLOF triggering and a 3-fold increase in the downstream area affected by potential GLOF paths under
70 future deglaciated conditions. Meanwhile, Zheng *et al.* (2021a) have elaborated such analyses for the entire High Mountain Asia, revealing that the number of lakes posing a transboundary threat within border areas of China and Nepal could double in the future (Zheng *et al.*, 2021a). While such large-scale, first-order studies are important for raising general awareness of the future challenges that mountain regions will face (Hock *et al.*, 2019), there are limitations in the extent to which these studies can directly inform planning and response actions at the ground level.

75 The need for forward-looking, anticipatory approaches to hazard and risk modelling, including attention to possible worst-case scenarios is clearly recognised within international guidelines on glacier and permafrost hazard assessment (GAPHAZ, 2017). However, practical examples on how to account for worst-case scenarios and future lake development in local GLOF hazard assessment and risk management have been rarely demonstrated. International best practice is framed by both a first-order
80 assessment undertaken at large scales (to identify potentially critical lakes), followed by a detailed assessment for these lakes using numerical models to simulate downstream flood intensities as a basis for hazard mapping (GAPHAZ, 2017). This is a common approach for existing threats, where the time, data, and expertise needed to invest in comprehensive hazard modelling and mapping can be well justified for a lake that is known to be critical, yet, worst-case scenarios are often neglected and may far exceed historical precedence. For future lakes, where the timing of lake formation is typically highly uncertain, there
85 remains a methodological gap in the hazard assessment process, as authorities are unlikely to undertake sophisticated hazard mapping for a threat that may not even eventuate. In this study we aim to address these gaps, by providing an illustrative example of how a worst-case outburst scenarios from a potential future lake can be systematically assessed along-side the threat posed by current lakes, before discussing the relevance of such an assessment for disaster risk management in a transboundary context.

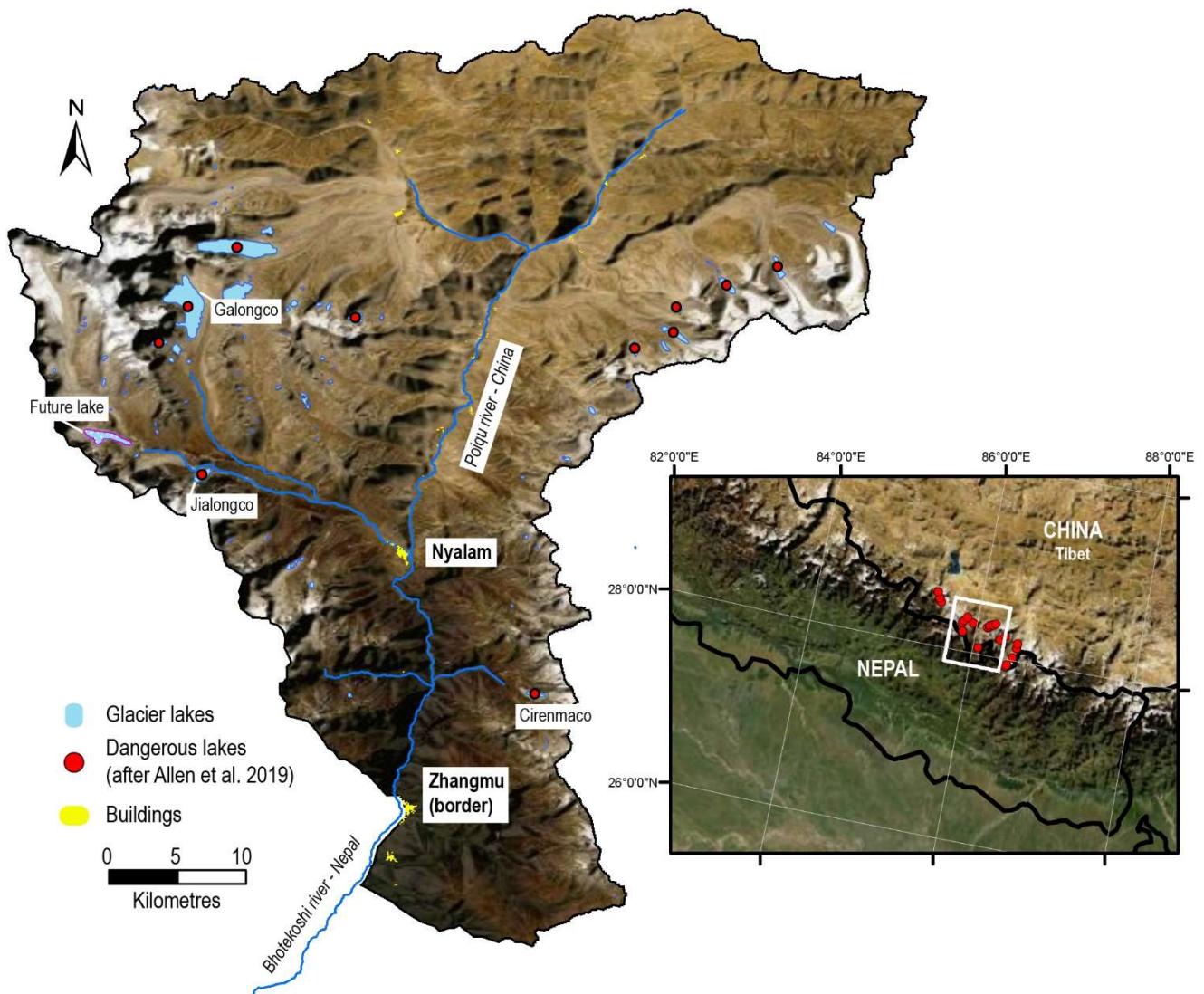
90 Focusing on the transboundary Poiqu river basin in the central Himalaya, the specific objectives of the study are to 1) apply systematic criteria to establish worst-case outburst scenarios and assess the magnitude of downstream impacts from two potentially critical lakes, considering also the effect of recent remedial measures at one of the lakes, 2) compare the results with a potential outburst from a large lake that is anticipated to develop in the future, and 3) discuss the implications for early
95 warning or other risk reduction strategies.

2 Study area

This analysis focuses on a ca. 40 km stretch of the lower Poiqu river basin originating from Galongco glacial lake, considering potential GLOF impacts in Nyalam town (capital of Nyalam county, Tibetan Autonomous Region), and downstream to the border with Nepal at Zhangmu (Fig. 1). The elevation range of the study area extends over 6000 metres, from the summit of Shishapangma at 8,027 m a.s.l, whose glacierised slopes feed Galongco, to 2000 m a.s.l in the river valley at Zhangmu. According to Wang and Jiao (2015), mean annual air temperature and mean annual precipitation in Nyalam (3810 m asl) are 3.8°C and 650.3 mm respectively, with sub-zero temperatures lasting from November – March each year. Temperatures peak in July (10.8°C), while highest average precipitation totals are recorded in September (87.9 mm). In total, 60% of the annual rainfall falls during the monsoon months of July – September (Wang *et al.*, 2015b)

The Poiqu basin is the Tibetan portion of the large transboundary Poiqu/Bhote Koshi/Sun Koshi River Basin, along which the economically important Friendship Highway links China to Nepal, and where significant hydropower resources are located (Khanal *et al.*, 2015b). Based on a larger study across Tibet, the Poiqu basin has been identified as a clear hotspot of transboundary GLOF danger (Allen *et al.* 2019 – Fig. 1), where at least 6 major GLOF events were reported over the past century, including repetitive events from Jialongco in 2002 (Chen *et al.*, 2013), and Cirenmaco in 1964, 1981 and 1983 (Wang *et al.*, 2018). The 1981 event resulted in numerous fatalities, and estimated losses of up to US\$4 million (currency value as of 2015) as a result of damage to houses, roads, hydropower, and disruption to trade and transportation services (Khanal *et al.*, 2015a). Meanwhile, an outburst of $1.1 \times 10^5 \text{ m}^3$ from Gongbatongshacuo (adjacent to Cirenmaco) in July 2016, resulted in significant damage to hydropower and roads, exacerbating losses inflicted one year earlier by the Gorkha earthquake (Cook *et al.*, 2018). Whereas Gongbatongshacuo has completely drained, Cirenmaco remains a persistent threat, identified by multiple studies as being one of the most dangerous lakes in Tibet (Allen *et al.*, 2019; Wang *et al.* 2015a; Wang *et al.*, 2018).

In the current study, we focus not on Cirenmaco, which has already been the subject of comprehensive investigations (Wang *et al.*, 2018), but rather on two other well-documented threats of Jialongco and Galongco, owing to their potential to cause damage to the Tibetan county capital of Nyalam, and downstream in Nepal (Allen *et al.* 2019; Shresta *et al.* 2010). In fact, after Cirenmaco, Galongco and Jialongco were ranked 2nd and 3rd respectively in a recent assessment of most dangerous glacial lakes across Tibet, owing to both the physical characteristics of the lakes and their surroundings (see section 4.1), and high levels of exposure in downstream areas (Allen *et al.* 2019). Both moraine-dammed proglacial lakes have expanded rapidly over the past decades, with Galongco, the largest lake in the basin, increasing its area by 450% from 1.00 to 5.46 km² in the period 1964-2017 (Wang *et al.*, 2015b; Zhang *et al.*, 2019). The potential future lake is located around 6 km further upstream from Jialongco (Fig. 1 – see 3.1 for further description).



130 **Figure 1: Location of the Poiqu River basin within a hotspot of GLOF risk, as determined on the basis of 30 potentially most dangerous lakes identified across Tibet (after Allen et al. 2019). The current lakes focussed on in this study of Galongco and Jialongco are indicated, as is the modelled future lake, the county capital town of Nyalam, and the town of Zhangmu, through which the border between China and Nepal passes. Cirenmaco, from which several outburst floods have been reported, is also indicated; Background image: ESRI Basemap Imagery.**

3 Methodological approach

135 In line with recent international guidance in GLOF hazard assessment (GAPHAZ 2017), in this study we consider lake susceptibility, which determines the likelihood of a given outburst scenario to occur, and use the GIS-based open-source numerical simulation tool *r.avaflow* to model the GLOF process chain and determine downstream impacts. In order to compare the threat posed by the two current lakes with an anticipated future lake, we focus on worst-case scenario modelling – that is to say, very large avalanche-triggered outburst events from Jialongco, Galongco, and the anticipated future lake.

140

3.1 Lake susceptibility and scenario development

The assessment follows a systematic approach that considers wide-ranging atmospheric, cryospheric and geotechnical factors that can influence lake susceptibility, and thereby the likelihood of a GLOF event occurring (after GAPHAZ 2017). We draw

on remotely sensed data to the extent possible, complimented with field observations to enable a semi-quantitative assessment and comparison of susceptibility factors across the three lakes. Topographic characteristics (dam geometry, slope angles etc) and geological structures of the surrounding slopes were precisely measured using high resolution 1m Pleiades orthoimagery and Digital Elevation Model (DEM), generated from 0.5 m resolution tri-stereo Pleiades imagery acquired in October 2018, covering the whole Poiqu basin. Potentially unstable zones of glacial ice were identified in the imagery and Google Earth, based on orientation and density of crevassing, with a subsequent estimate of the ice thickness and volume provided from GlabTop model output (Table 1). Furthermore, the time series of Google Earth imagery was examined to identify any evidence of historical mass movements, that could indicate an enhanced threat to the lakes below. Factors assessed, their primary attributes, and sources used are further described in Section 4.1. Based on this assessment, and the recognition of a large ice and/or rock avalanche triggered GLOF process-chain being the most significant threat to all 3 lakes, avalanche source areas were identified as input to the process chain modelling (Table 1).

Table 1: Input scenarios for rock/ice avalanche starting zones (see Fig. 2) threatening Jialongco (JC), Galongco (GC), and the future lake (FL). Source areas are defined based on high-resolution satellite imagery. Mean ice thickness and resulting ice volume is based on GlabTop. Note that the JC-L scenario is defined for a lowered Jialongco lake, as the lake level was lowered since 2018; See Section 4.1 for further details.

	Mean slope (°)	Area (m ²)	Type	Mean ice thickness (m)	Ice volume (10 ⁶ m ³)	Mean rock thickness (m)	Rock volume (10 ⁶ m ³)	Total volume (10 ⁶ m ³)
JC	35	600,000	Ice avalanche	30	18 (100%)	-	-	18
JC-L	35	600,000	Ice avalanche	30	18 (100%)	-	-	18
GC	50	460,000	Rock-ice avalanche	10	4.6 (20%)	40	18.4 (80%)	23
FL	55	516,000	Rock avalanche	-	-	40	20.6 (100%)	20.6

3.2 Avalanche and GLOF Modelling

The GLOF process chain was simulated with r.avaflow (Mergili et al., 2017; Pudasaini and Mergili, 2019), a GIS-based open-source simulation framework for multi-phase mass flows, which has the capacity to dynamically compute the interaction between triggering landslides (in this case rock/ice avalanches) and lakes. The model is also capable of computing debris flow hydraulics. Major model inputs include the initial avalanche source characteristics (Table 1), terrain data, friction parameters and erosion parameters (see below), lake bathymetry and volume.

Bathymetry surveys of Jialongco and Galongco were undertaken in 2019, using an unmanned vessel. The onboard GPS system achieves ~2.5 m horizontal positioning accuracy, while the single-beam sonar sounder has a vertical accuracy of 1 cm ± 0.1% of depth measured. Contour maps of lake depths were interpolated by using Kriging geo-statistics. Maximum depths of 134 and 200 metres were recorded for Jialongco and Galongco respectively, while volumes based on the interpolated bathymetry were 40 and 590 x 10⁶ m³. Following the construction of an artificial channel and associated lowering of the water level in Jialongco, bathymetry was remeasured in 2021, giving a post-lowering maximum depth of 113 m, and volume of 23.5 x 10⁶ m³.

For GLOF modelling from the future lake, the location, bathymetry, and volume of the potential lake upstream from Jialongco
180 is based on a modelled overdeepening in the glacier bed topography using GlabTop (Linsbauer *et al.*, 2012). The model is now
well established for providing a first-order indication of where lakes may develop in the future (e.g., Allen *et al.*, 2016; Haeberli
et al., 2016a; Linsbauer *et al.*, 2016; Magnin *et al.*, 2020). The ice thickness distribution from GlabTop is subtracted from a
surface DEM to obtain the bed topography, i.e. a DEM without glaciers, from which overdeepenings in the glacier bed can be
detected and volumes estimated. Inputs to the model include manually edited glacier branch lines, and a DEM – in this case
185 the NASA Shuttle Radar Topography Mission (SRTM) Version 3.0 (void filled) was used, at 30 m resolution. While the model
predicts several possible locations in the Poiqu basin where large future lakes can develop, we focussed on the largest of these
lakes that threaten the town of Nyalam. Based on the modelled geometry of the overdeepening, a maximum future lake depth
of 168 m, and volume of $70 \times 10^6 \text{ m}^3$ is estimated. The modeled bedrock topography forms the lake dam, i.e., the possible
deposition of moraine on top of the bedrock, creating a higher dam structure, is not considered. Likewise, in keeping with a
190 worst-case approach, we do not consider sediment deposition into the lake, that will potentially reduce the volume and
longevity of the lake (Steffen *et al.* 2022). Beyond its potential size, this overdeepening was selected owing to its position in
an area of low surface gradient behind a pronounced terminal moraine, beneath a tongue where supraglacial ponds are already
developing, and at an elevation that is lower than other overdeepenings in the area. All factors provide favourable
preconditioning for the formation of a large proglacial lake (Frey *et al.*, 2010; Linsbauer *et al.*, 2016).

195

Depending on the defined GLOF process-chain scenarios (Table 1), we assume the mixture of one or two solid phases in the
initial avalanche (rock component; $\rho=2700 \text{ kg/m}^3$ and ice component; $\rho=900 \text{ kg/m}^3$) and one fluid phase; $\rho=1000 \text{ kg/m}^3$ (lake
water), where the ice-rock volume ratios are calculated based on assessment in Section 4.1. We define the damming moraine
of the lakes as entrainment zones composed of the rock phase (representing glacier deposits) with a grain density of 2700
200 kg/m^3 . A simplified entrainment model is applied, which is a product of the flow momentum and the empirical entrainment
coefficient (Mergili *et al.*, 2017). However, the final erosion depths are dependent on the momentum of the particular process
and are controlled by the entrainment coefficient. Other input parameters include basal friction angle (φ) and internal friction
angle (δ) that govern the rheology of the flow. Here we set $\varphi = 25^\circ$, $\delta = 10^\circ$ for the initial stage of the process chain dominated
mostly by the solid phase, i.e., avalanche, lake impact, and moraine erosion. For the downstream process from the moraine,
205 we set $\varphi = 25^\circ$, $\delta = 1^\circ$ to model the flow as a water-saturated debris flow. The domain of the model is constructed such that it
completely encompasses the avalanche source areas down to the China-Nepal border. All the simulations are executed for a
total duration set to 1 hour 15 minutes (4500 s) providing enough time to evaluate the GLOF propagation downstream to the
border. Finally, to evaluate the flow hydraulics obtained in terms of flow depth and discharge; we define three cross-sections
along the flow channel located (i) immediately downstream of the damming moraine (ii) at Nyalam (nearest settlement), and
210 (iii) at Zhangmu (China - Nepal border).

It is to be noted that we assumed no entrainment of the frontal moraine in the Jialongco Lowered Scenario (JC-L), as the
damming moraine was lowered by up to 15 – 20 m, and armoured with concrete as a part of the engineering works performed
for GLOF mitigation since 2018. For GLOFs originating from the future lake we evaluate the cascading impact of the flow
impacting into Jialongco, located ~6 km downstream (see Fig. 1). While several freely available DEMs were tested (e.g.,
215 ALOS PALSAR at 12.5 m or HMA at 8 m), topographic artefacts led to modelling errors. As such, the 1-m Pleiades DEM
was finally used for all simulations (based on imagery from 2018, with exception of the JC-L simulation which used an updated
DEM from 2021 for the dam area).

3.3 Future lake development

220 Previous studies (e.g. Quincey *et al.*, 2007; King *et al.*, 2018) have identified glacier surface attributes which may precondition the surface of debris-covered glaciers for supraglacial lake development. Glaciers bounded by large lateral and terminal moraines which have a flat or gently sloping ($< \sim 2^\circ$), slowly flowing ($< \sim 10 \text{ m a}^{-1}$) main tongue are hotspots of supraglacial pond development as surface meltwater cannot drain from the glacier surface (e.g. Quincey *et al.*, 2007; King *et al.*, 2018). Such pond networks expand when the mass balance of the glacier is negative and coalesce to eventually form a supraglacial
225 lake at the hydrological base level of the glacier- the lowest point where the glacier surface intersects the terminal moraine (Figures 3 & 19 in Benn *et al.*, 2012). Large supraglacial lakes located close to the termini of debris-covered glaciers can persist for decades, over which period they expand, deepen and eventually transition to become proglacial lakes, such as Galongco and Jialongco. By examining contemporary and historical glacier surface velocity and elevation changes it is therefore, possible to identify glacier surfaces suited for surface meltwater ponding, which represent current and future sites
230 of supraglacial lake development. To establish the possibility of lake development and the likely future trajectory of lake area growth on the parent glacier up-valley from Jialongco (RGI60-15.09475), we examined the surface velocity, rate of thinning, and the evolution of the geometry (surface slope) of the glacier in recent decades.

We used the Pleiades DEM and glacier surface elevation change data generated by King *et al.* (2019) to examine the evolution
235 of the geometry of glacier RGI60-15.09475 since the 1970s. Glacier surface slope estimates were derived by the fitting of linear regression models through 'average' (mean of 5 evenly spaced) elevation profiles of the glacier surface split into 750 m long segments (King *et al.*, 2018). We also assessed the current flow regime of the glacier using surface velocity data, which was generated through the tracking of glacier surface features visible in Sentinel 2 imagery over the period 2017-2019 (Pronk *et al.*, 2021). Examination of these parameters established that the conditions at the surface of the glacier (Fig. 7) are well
240 suited to imminent glacial lake development considering the factors outlined by Quincey *et al.* (2007), namely low ($< 2^\circ$) surface slope, negligible ice flow ($< 10 \text{ m a}^{-1}$) and sustained glacier thinning.

To investigate the likely size of such a lake in the coming decades we consider two different scenarios of glacier thinning between 2015 and 2100 and follow a similar method to that of Linsbauer *et al.* (2013) to simulate glacier thickness into the
245 future, but employ different criteria to determine future lake area. Our first scenario is based on the assumption that the acceleration in glacier thinning in the Poiqu basin measured by King *et al.* (2019) is replicated by the year 2100. Such an increase in thinning will be driven by a further 1°C increase in temperature by 2100 (Kraaijenbrink *et al.*, 2017), further to the $\sim 1^\circ\text{C}$ increase in temperature which has occurred in the central Himalaya (Maurer *et al.*, 2019) since the 1970s. The second scenario is based on the premise that the increase in thinning which has occurred between 1974 and 2015 will be replicated
250 over subsequent equivalent time periods (by 2056, 2097, etc). We extrapolated the thinning rates from King *et al.* (2019) and integrated the resulting elevation changes between 2015 and 2100. We then assumed that once the glacier surface had lowered to a height below the hydrological base level of the glacier (4890 m a.s.l.), meltwater ponding would occur and that DEM pixels with an elevation of less than this threshold represented lake area at that point in time.

4 Results

255 For Jialongco, Galongco and the potential future lake, we focus below on results relating to the susceptibility of the lakes to produce an outburst event, and the potential magnitude of downstream impacts, as simulated under worst-case scenarios. A full hazard and risk assessment, including a complete range of outburst scenarios and vulnerability mapping, is beyond the scope of this study.

4.1 Lake susceptibility and scenario development

260 The susceptibility component of GLOF hazard assessment establishes the likelihood of an event from a given lake, considering the wide-ranging factors that can condition or trigger an outburst. The likelihood (which can be both qualitative or quantitative for some hazards) is always specific to a given magnitude and valid for a given time frame, recognising that susceptibility can evolve over time (Allen *et al.* 2021). Based on this assessment, scenarios for hazard modelling can be established, including worst-case outburst scenarios as we focus on here. Taking a systematic approach (after GAPHAZ 2017), we compare the relative susceptibility of the three lakes considered in this study, considering also how this susceptibility might evolve in the future (Table 2). The table distinguishes those factors that condition and/or trigger an outburst event, while also linking to those factors that inform about possible outburst magnitudes.

270 Located in a transitional zone to the north of the main Himalayan divide, the upper Poiqu basin is subject to heavy rainfall during the Asian summer monsoon. With a significantly larger watershed area, Galongco is considered more susceptible to heavy rain and/or snow melt leading to high lake water levels, and under future deglaciated conditions the lake may become fed by a well-developed paraglacial stream network. However, even under these conditions, the relatively favourable dam geometry (low width to height ratio and 15 m dam freeboard) suggests that the likelihood and magnitude associated with an outburst via this triggering mechanism is low. Similarly, self-destruction via warm temperatures and melting of ground ice within the moraine dam is extremely unlikely. Creeping permafrost features visible in the vicinity of Galongco, modeled mean annual ground surface temperature (MAGST) (after Obu *et al.* 2019) and a partially hummocky appearance of the lake dam, suggests a strong likelihood of a partially ice-cored moraine, but the huge width (> 200 m) and gentle downstream slope of the dam would make a catastrophic failure in the case of thawing extremely unlikely.

280 As with the majority of large glacial lakes across the Himalaya (Liu *et al.*, 2013; Richardson and Reynolds, 2000; Sattar *et al.*, 2021), the main triggering threat is considered to come from large slope instabilities, impacting into the lake. Under current conditions, Jialongco is assessed to be most susceptible to ice avalanches, given the presence of a steep, highly crevassed tongue positioned directly behind the lake (Fig. 2a). With an average slope of 35°, large transverse crevasses marking a sharp break in topography, and likely temperate conditions at the bed, full collapse of the glacier tongue ($\sim 18 \times 10^6 \text{ m}^3$) is considered a feasible worst-case scenario (Table 1). The mass would impact the lake in a direction parallel to the longitudinal axis of the lake, leading to maximum overtopping wave heights and swashing effect. Smaller ice avalanches from this glacier have triggered GLOFs from Jialongco in 2002, at a time when the lake was less than half of its current size (Chen *et al.* 2013). While climate warming is expected to increase temperatures and meltwater at the glacier bed (Kääb *et al.* 2021), potentially reducing the stability of the glacier, warming-driven retreat of the tongue will see a reduction in the potential avalanche volume over time, and eventually, this threat will be eliminated completely as the ice retreats to a flatter plateau. In comparison, the partially debris-covered parent glacier tongue of Galongco has a gentle mean slope (18°) and uniform gradient. Potential unstable ice masses threatening Galongco, from steep ice cliffs and hanging glaciers, are found higher up on the mountain (Fig. 2b), with estimated maximum volumes in the range of $0.1 - 1 \times 10^6 \text{ m}^3$. Avalanches from the larger of these starting zones would strike the lake perpendicular to the longitudinal axis of the lake (from the west) meaning most of the energy from a displacement wave would be dissipated on the opposing side of the lake. It is a similar situation above the future lake, where small, and comparatively thin hanging glaciers are restricted to the slopes southwest of the potential lake (Fig. 2c).

Hence, a large rock or combined ice-rock avalanche is considered to be the most feasible mechanism capable of triggering a worst-case GLOF from either Galongco or the potential future lake. The northeast-facing slopes of Shishapangma rise nearly

300 3000 m above Galongco, and are likely to be mostly underlain by cold permafrost conditions. This is inferred both from the distribution of rock glaciers in the region, extending down as low as 4000 m a.s.l (Bolch *et al.* 2022), and modelled MAGST (Obu *et al.* 2019) (Table 2). However, the presence of ice cliffs and hanging glaciers can lead to thermal perturbations, and even melt conditions in otherwise very cold environment (Shugar *et al.* 2021). Based on close examination with high-resolution imagery, a large potential starting zone extending from 6550 – 7340 m a.s.l was identified on a heavily fractured slope beneath the south ridge of Shishapangma (Fig. 2b). Here, as in the surrounding peaks, layered leucogranite sits above sillimanite gneisses with a gentle northerly dipping schistosity (Searle *et al.* 1997). The slope has been eroded and potentially oversteepened by the glacier below. Based on structures outcropping on the face, a 40 m maximum bedrock depth was assumed, while steep ice cliffs and firn covering the slope is estimated to not exceed 10 m, resulting in a combined starting volume of $23 \times 10^6 \text{ m}^3$ (20% ice and 80% rock). The potential future lake is positioned directly beneath the ice-free ~ 2000 m high eastern face of Ramthang Karpo Ri (Fig. 2c), where MAGST is in the range of $-3^\circ\text{C} - -6^\circ\text{C}$. The face is dissected by numerous vertical structures and there is evidence of several scarps from previous instabilities. A large potential source area was identified, comparable to the Galongco scenario, with scarps on the face suggesting similar maximum depths of up to 40 m, leading to a total rock avalanche volume of $20.6 \times 10^6 \text{ m}^3$ (Table 1).

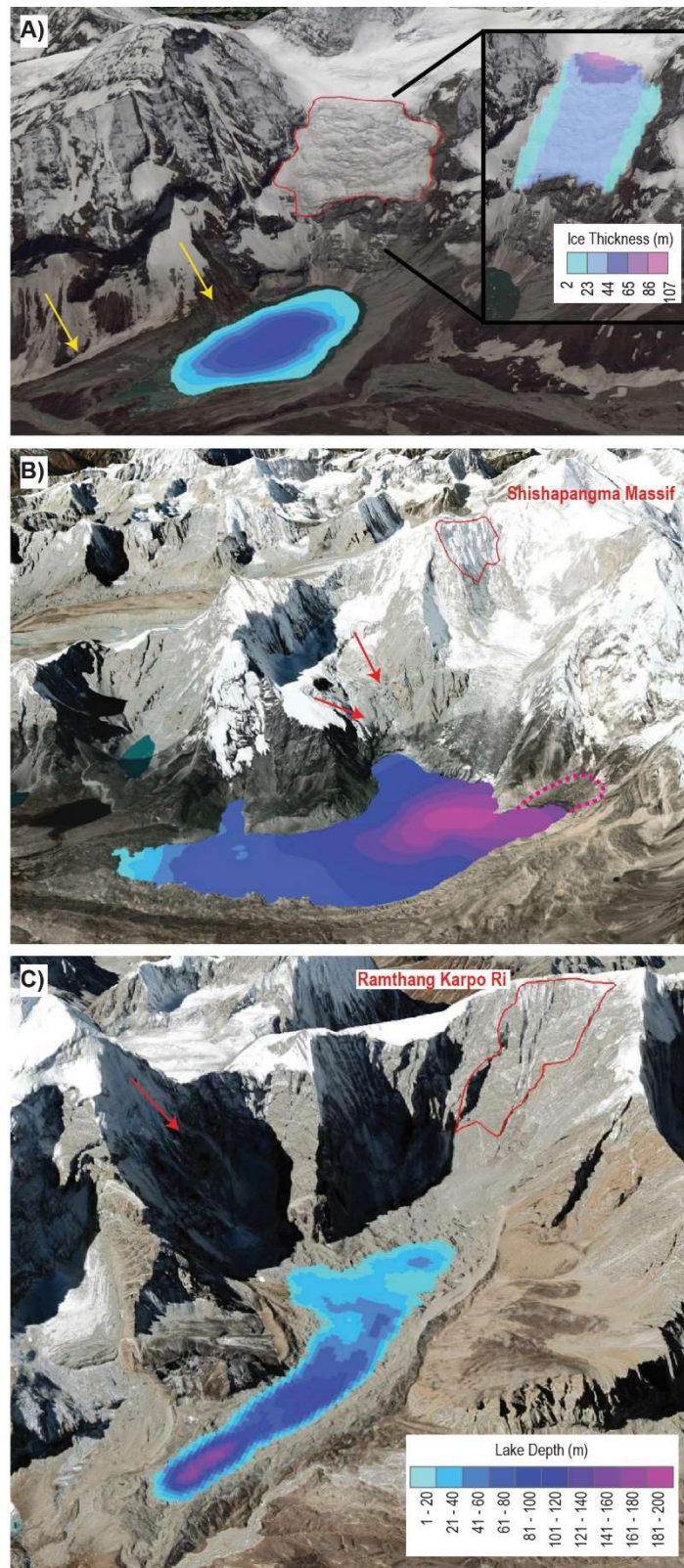
315 Even on a global scale, ice and/or rock avalanche volumes of the magnitude included in the scenarios here are rare (Kääb *et al.*, 2021; Schneider *et al.*, 2011), although have occurred recently (Shugar *et al.* 2021) and prehistorically (Stolle *et al.* 2017) in the Himalaya. While Poiqu basin is located within a high seismic hazard zone (Shedlock *et al.*, 2000), it is notable that the 2015 Gorkha earthquake did not cause any large ice/rock avalanches in the Poiqu basin, despite significant damage in Nyalam and along the highway to Nepal (Kargel *et al.* 2016). Hence, given a lack of historical large instabilities in the basin, ice/rock avalanches of the magnitude included in this study are assessed to be low to very low likelihood events (see also Section 5 - discussion). Geologically there is little basis for distinguishing the likelihood of bedrock failures above the three lakes, and permafrost conditions are comparable (Table 2). Owing to the position of Jialongco directly beneath a steep glacier tongue, history of ice-avalanche triggered outburst events, and more unfavourable dam conditions (low freeboard, narrow width), we assess a worst-case outburst from this lake to be more likely than from Galongco under current conditions. Finally, all three lakes are or will be susceptible to instantaneous or progressive landslides occurring from the adjacent lateral moraines, most notably for Jialongco where active instabilities are clearly evident (Fig. 2a). Recent studies have shown that large lateral failures, either instantaneous or progressive, can be sufficient to initiate catastrophic process chains where dam geometries are sufficiently prone to erosion (Zheng *et al.*, 2021b).

330 **Table 2: First-order lake assessment of wide-ranging factors determining the susceptibility of glacial lake (based on GAPHAZ 2017). Colours represent an expert assessment of high (orange), moderate (yellow), and low (green) susceptibility for each of the factors considered. No colour indicates the factors were not considered relevant for these lakes. Factors can be relevant for conditioning (con.) and/or triggering (trig.) a GLOF, and can also have an influence on outburst magnitude (mag.).**

Susceptibility factors for GLOFS	Relevance			Relevant Attributes	Susceptibility			Assessment methods and sources
	Con.	Trig.	Mag.		Jialong Co	Galong Co	Future lake	
a) Atmospheric								
Temperature	+	+		Mean temperature	Increasing	Increasing	Increasing	Climate observations and projections (Ren <i>et</i>

				Intensity and frequency of extreme temperatures	Increasing	Increasing	Increasing	<i>al., 2017; Sanjay et al., 2017)</i>
Precipitation	+	+	+	Intensity and frequency of extreme precipitation events.	Increasing	Increasing	Increasing	
b) Cryospheric								
Permafrost conditions	+	+		State of permafrost, distribution and persistence within lake dam area and bedrock surrounding slopes	No permafrost in dam area (MAGST > 1°C). Degrading permafrost in surrounding headwalls (< -3°C).	Likely ice-cored moraine dam (MAGST - 1°C). Degrading permafrost in surrounding headwalls (< -4°C).	Possible permafrost in dam (MAGST - 0.5 - -1°C). Degrading permafrost in surrounding headwalls (-3°C - -6°C).	Model-based results (Schmid <i>et al.</i> , 2015; Obu <i>et al.</i> 2019); Google Earth
Glacier retreat and downwasting	+		+	Enlargement of proglacial lakes, enhanced supraglacial lake formation, dam removal or subsidence	Lake currently at maximum extent. Glacier not in contact with lake.	Minimal potential for further expansion (+1%).	Lake will be actively expanding over several decades, as overdeepening emerges.	GlabTop; Landsat archive (Zhang <i>et al.</i> 2019); Google Earth; DEM differencing (King <i>et al.</i> , 2019)
Advancing glacier (incl. surging)	+			Formation of ice-dammed lakes	Not relevant	Not relevant	Not relevant	Google Earth
Ice avalanche potential		+	+	Steep glacier tongue or ice cliffs, crevasse density and orientation, ice geometry	High potential Steep heavily crevassed glacier tongue. Likely past events triggering a GLOF.	Moderate potential Considerable steep cliff ice and small hanging glaciers.	Low potential. A few small hanging glaciers.	GlabTop; DEM slope analyses; Google Earth
Calving potential		+	+	Width of glacier calving front, activity, crevasse density	Glacier not in contact with lake.	Minimal potential (calving front = 300 m).	High potential (calving front = > 1km).	Google Earth
Lake size	+		+	Area, volume, and/or depth	Mean depth: 64 m (lowered to 48 m) Volume: 40 (reduced to 23.5) x 10 ⁶ m ³	Mean depth: 108 m Volume: 590 x 10 ⁶ m ³	Mean depth: 46 m Volume: 70 x 10 ⁶ m ³	Field based bathymetry; GlabTop for future lake
c) Geotechnical and Geomorphic								
Dam type	+		+	Bedrock, moraine, ice	Moraine, now partially armored.	Moraine	Moraine	Google Earth
Dam width to height ratio	+		+	Width across the dam crest relative to the dam height	4:1 (engineered now to 8:1)	9:1	8:1 (large uncertainty)	Google Earth; High resolution DEM analyses (Pleiades)
Freeboard (measured from the crest of the dam to the lake water level,	+		+	Elevation difference between lake surface and	~ 20 m (engineered now to ~ 10)	~ 15 m	~ 10 m (large uncertainty)	Google Earth; High resolution DEM analyses (Pleiades)

irrespective of any outflow channel)				lowest point of moraine.				
Downstream slope of dam	+			Mean slope on downstream side of lake dam.	Artificially armored channel	10°	20° (large uncertainty)	Google Earth; High resolution DEM analyses (Pleiades)
Vegetation on dam	+			Density and type of vegetation (grass, shrubs, trees).	Partially armored. Grass/scrub in other areas.	Absent	Absent	Google Earth
Catchment area	+			Total size of drainage area upstream of catchment	9 km ²	35 km ²	10 km ²	DEM analyses
Catchment mean slope	+			Steepness of catchment area	32°	28°	29°	DEM analyses
Catchment drainage density	+			Density of the stream network in catchment area	Low density stream network to develop under deglaciated conditions.	Moderate density stream network to develop under deglaciated conditions.	Low density stream network to develop under deglaciated conditions.	GIS based hydrological modelling
Catchment stream order	+			Presence of large fluvial streams, facilitating rapid drainage into lake	Low order streams to develop in future	Moderate order streams to develop in future	Low order streams to develop in future	GIS based hydrological modelling
Upstream lakes	+			Presence and susceptibility of upstream lakes.	None currently. Two small lakes (~0.01 km ²) anticipated in future.	None currently or anticipated in future.	None currently or anticipated in future.	GlabTop; Google Earth
Rock avalanche potential		+	+	Steep, structurally unstable bedrock slopes with potential to runout into the lakes.	Steep, heavily fractured slopes. Recent instabilities not evident. Scarps indicative of prehistoric failures.	Steep, extensively glaciated slopes. Recent instabilities not evident. Scarps indicative of prehistoric failures.	Steep, heavily fractured slopes. Recent instabilities not evident. Scarps indicative of prehistoric failures.	GIS-based topographic potential modelling; Google Earth and high resolution imagery.
Moraine instabilities		+	+	Potential for landslides from moraine slopes into the lake	Steep moraine and talus slopes > 400 m high. Large instabilities evident.	Steep moraine slopes 100 – 200 m high. Minor instabilities evident.	Steep moraine slopes in the order of 100 – 200 m anticipated.	Google Earth
Seismicity		+		Peak ground acceleration	Very High 5.1 m/s ²	High 4.1 m/s ²	Very High 4.6 m/s ²	Global Seismic Hazard Map (Shedlock <i>et al.</i> , 2000)



340 **Figure 2: Rock/ice avalanche starting zones (in red) used as input scenarios for the modelling of outburst flood process chains from the 3 lakes (see Table 1 for details). A) Jialongco: The inset shows the GlabTop modelled ice thickness of the ice avalanche source area, and yellow lines indicate the steep lateral moraine walls also threatening the lake (see also Figure 9). B) Galongco: Large rock/ice avalanche source area outlined in red, while arrows indicate smaller sources areas of unstable ice, with possible future**

expansion of the lake shown by the dashed line. C) Projected future lake: Large rock avalanche source area outlined in red, while arrow indicates possible source area of smaller ice avalanches. Measured (and interpolated) lake bathymetry is shown in A and B, with modelled bathymetry of the future lake (C) derived from GlabTop. Background imagery from Google Earth.

4.2 GLOF modelling

Worst-case outburst scenarios for the three lakes were simulated until the border between China and Nepal (town of Zhangmu). The modeled flow does not extend beyond the border owing to the limited coverage of the required high-resolution Pleiades DEM. Of the two current lakes assessed, the modeled peak discharge from Galongco is more than 5 times larger than that from Jialongco, leading to flow depths up to 14 m higher impacting the town of Nyalam (Table 3, Figs. 3 and 4). At the border, 20 km downstream, inundation depths are up to 17 m higher for the Galongco simulation as the large volume of water becomes constricted in the narrow topography of the valley, with discharge values remaining above $100,000 \text{ m}^3 \text{ s}^{-1}$ even after 1 hour (Fig. 3). The simulated worst-case outburst from the potential future lake has a calculated peak discharge at the dam of $359,628 \text{ m}^3 \text{ s}^{-1}$, resulting in flow depths (27 m) and discharge ($163,667 \text{ m}^3 \text{ s}^{-1}$) in Nyalam that would exceed that of Jialongco, but are an order of magnitude lower than from Galongco. Differences in the shape of the outflow hydrographs at the dam (Fig. 3a), and travel distance, lead to minor variations in the arrival of the modelled flood waves in Nyalam and further downstream at the border with Nepal. The flood wave from Jialongco first registers after 6 minutes in Nyalam, with the maximum flow heights arriving 2 minutes later (all times relative to the initial avalanche release). In contrast, the flood wave from Galongco first registers after 10 minutes, with maximum flow heights arriving 4 minutes later. An outburst from the potential future lake has a similar arrival time of only 11 minutes in Nyalam, while all simulated outbursts reach the Nepalese border within a range of 28 - 32 minutes after the avalanche release. Notably, the remedial measures undertaken at Jialongco, which result in a larger initial peak discharge and lower debris entrainment (due to lowering and armouring of the lake dam), result in a worst-case GLOF that attenuates at a slower rate (54% decrease in discharge between Nyalam and Zhangmu) compared to the simulation for the original lake (81% decrease in discharge between Nyalam and Zhangmu) (Fig 3).

Potential processes that could further enhance the GLOF magnitude include entrainment of large volumes of sediment along the flow path leading to additional bulking of the flow volume, blockages of a river by GLOF deposits leading to secondary outburst events, and a process chain involving more than one lake. Significant erosion of sediment from within the main river channels is considered unlikely for any of the three outburst scenarios, given that average trajectory slope angles measured along the flow paths are well below those needed to entrain sediment from within a channel (Huggel *et al.*, 2004). However, undercutting, erosion and destabilisation of the river banks as a result of the GLOF means that such secondary hazards cannot be excluded, particularly in the steep sided gorge downstream of Nyalam. Immediately below Nyalam, the valley narrows, leading to pooling of water in the simulations, and a backwash effect is produced that extends 2 km up the Poiqu river, with maximum flow depths of $>60 \text{ m}$ under the Galongco scenario (Fig. 3a). Significant deposition of sediment can be anticipated within this backwash zone, with the potential to block the Poiqu river and form a major secondary hazard, in line with processes observed and modelled during the 2021 catastrophic mass flow in Chamoli, northern India (Shugar *et al.* 2021).

380

Table 3: Measured and modelled lake and outburst flood parameters for Galongco (GL), Jialongco pre-lowering (JC), Jialongco post-lowering (JC-L), and the future lake (FL). All timings are relative to the start of the initial rock and/or ice avalanche.

	GL	JC	JC-L	FL
Lake area (km ²)	5.46	0.62	0.49	1.54
Mean lake depth (m)	108	64	48	46
Lake volume (10 ⁶ m ³)	590	40	23.5	70
GLOF peak at dam (m ³ s ⁻¹)	585,686	92,421	101,919	359,628
Time of arrival at Nyalam	10 min	5 min	6 min	11 min
Flow depth at Nyalam (m)	37	23	23	27
Flow discharge at Nyalam (m ³ s ⁻¹)	221,655	64,124	77,695	163,667
Time of arrival at Zhangmu	28 min	32 min	28 min	30 min
Flow depth at Zhangmu (m)	29	7	12	14
Flow discharge at Zhangmu (m ³ s ⁻¹)	170,404	12,251	35,389	54,656

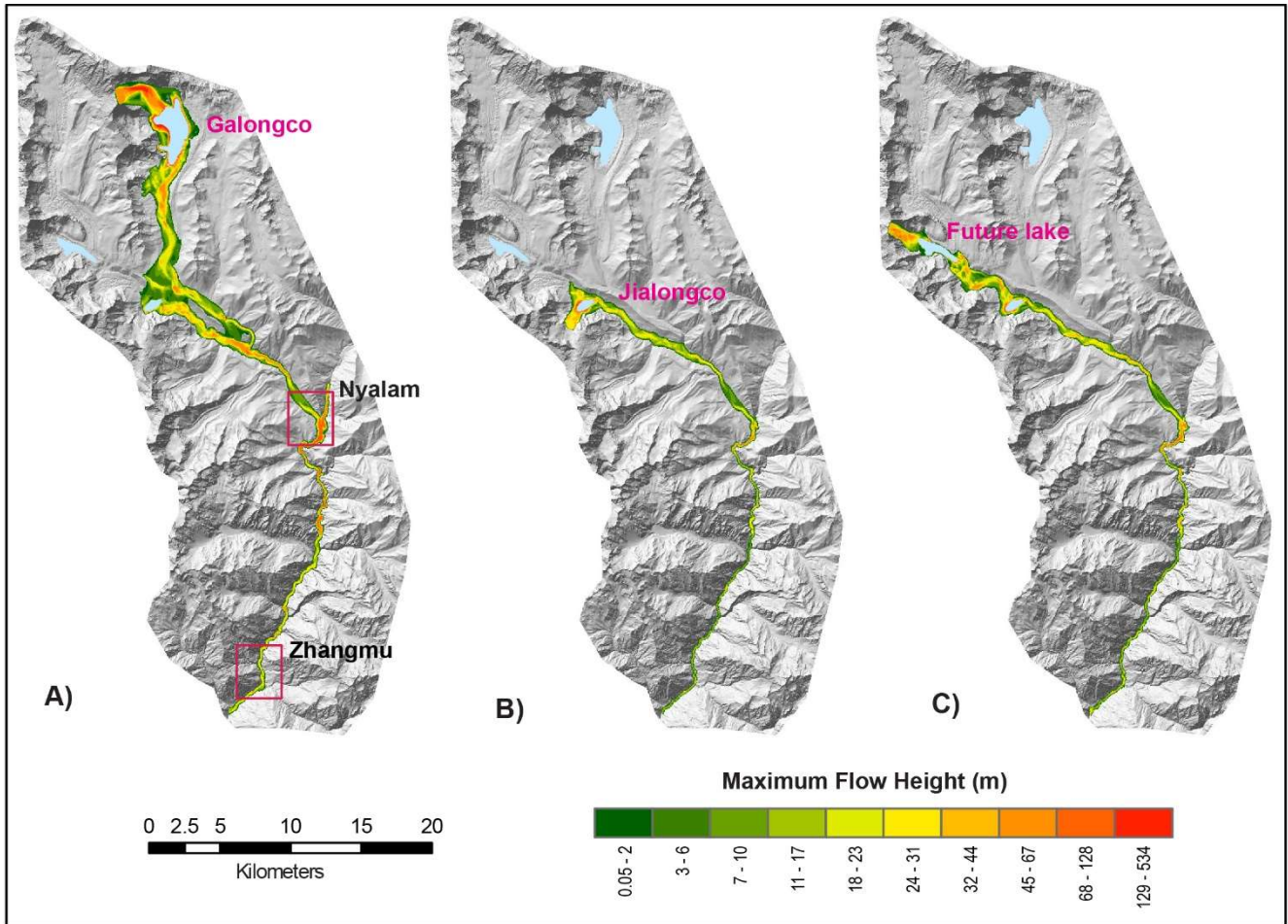
385

In contrast to previous modelling results for Galongco (Shrestha *et al.* 2010; Zhang *et al.* 2021), the worst-case avalanche triggered GLOF path is not confined to the existing river channel, overtopping the orographic-right side of the valley (bounded by old moraines) and spilling over into Jialongco to form a second, larger flow path towards Nyalam (Fig. 3a). The two paths converge again about 6 km upstream from Nyalam. The hyper-elevation of the flow that enables this overtopping is consistent with observations of catastrophic mass flows of comparable magnitudes (Shugar *et al.* 2021). Results further indicate that an outburst event from the potential future lake could slam into, pool up, and eventually overtop the lateral moraine of Jialongco, producing a potential chain reaction where Jialongco also breaches (Fig. 5). Despite adding volume to the flow, the presence of Jialongco with its prominent lateral moraine acts as a topographic obstruction that slows and reduces the energy of the outburst event, with a 50% reduction in discharge values measured immediately upstream and downstream of Jialongco. Although only one specific cascading lake interaction, this example highlights that lakes positioned downstream of another lake do not necessarily increase GLOF hazard, depending upon the downstream lake geometry and its orientation relative to the incoming GLOF path.

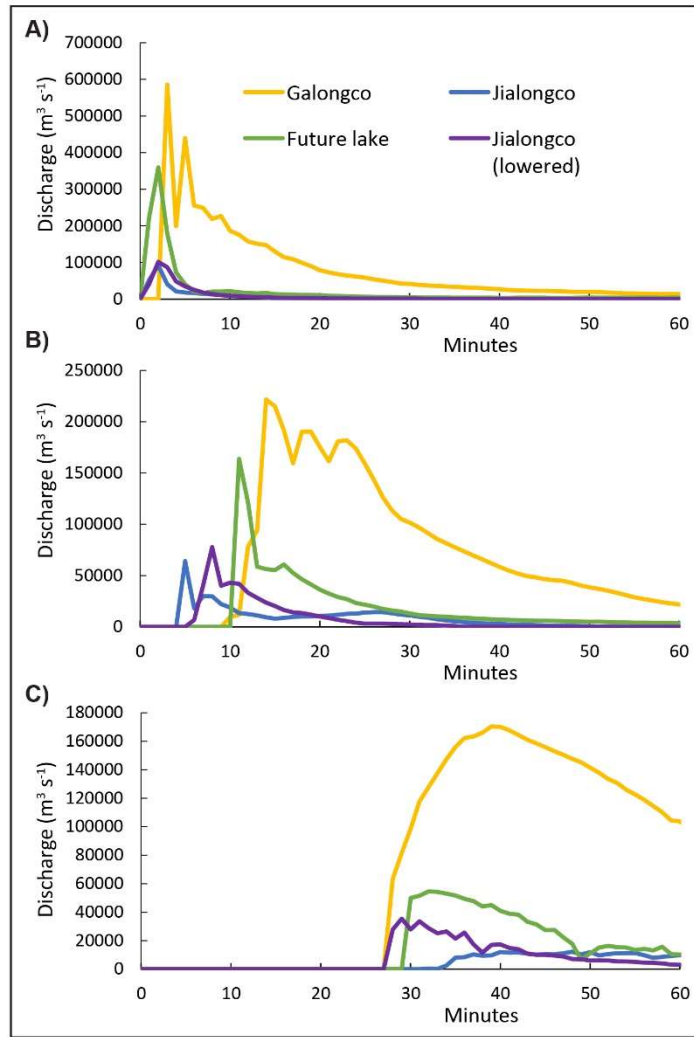
390

395

400

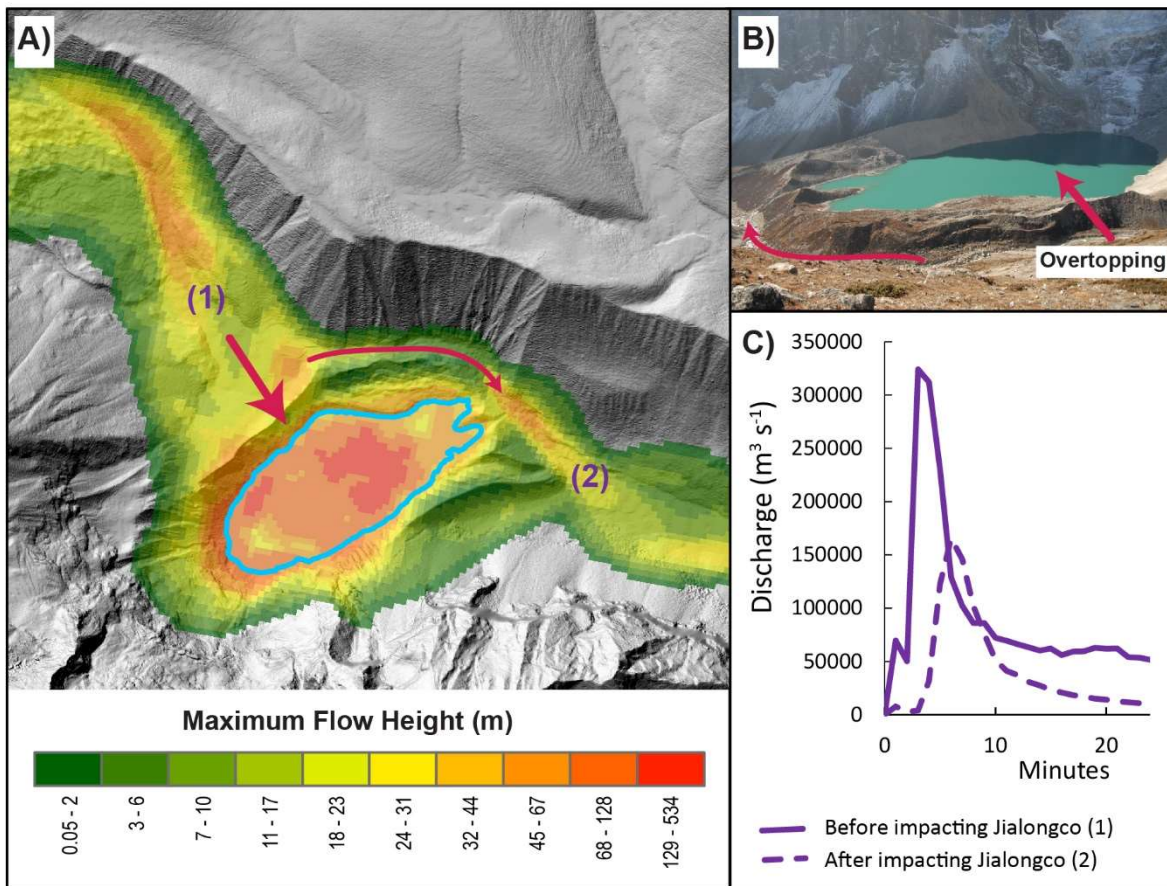


405 **Figure 3: Modelled GLOF flow heights for worst-case scenarios from A) Galongco, B) Jialongco (JC-L), and C) the potential future lake. The location of Nyalam and Zhangmu towns are indicated by the red boxes in (A) .**



410

Figure 4: A) Modelled GLOF discharge for three assessed lakes taken at A) the lake dam, B) Nyalam and C) Zhangmu.



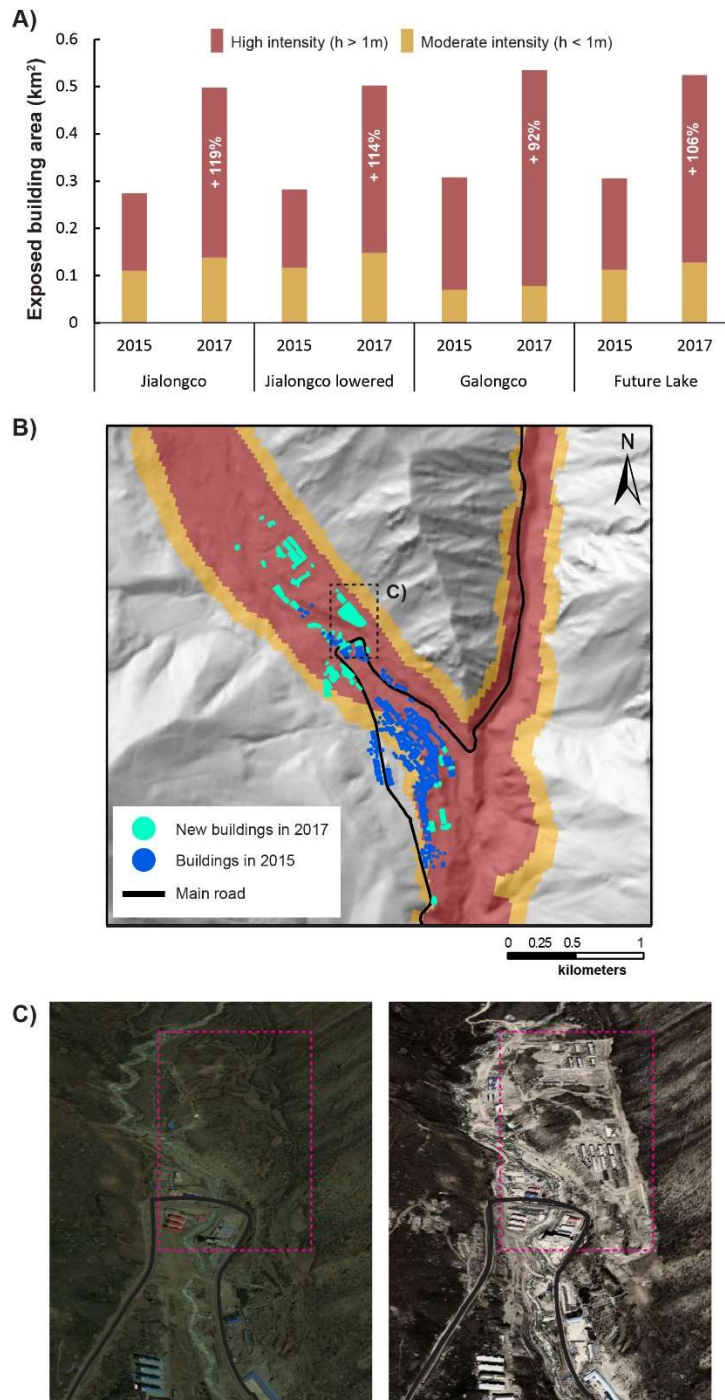
415

Figure 5: A) Modelled GLOF flow heights for an outburst event from the potential new lake, showing area of pooling and
 420 height at the point where overtopping is illustrated in the photo (B) is around 40 m (Photo: O. King, October 2018). C) Flow
 hydrographs immediately upstream (1) and downstream (2) of Jialongco are simulated with r.avaflow. Note that the simulation is
 based on the post-lowering lake bathymetry and dam geometry of Jialongco (JC-L).

4.3 GLOF impact and exposure

425 We identify from Open Street Map and Google Earth imagery, the buildings in Nyalam exposed to different GLOF intensity
 levels according to simulated debris flow intensities (after GAPHAZ 2017). While classification schemes vary across
 countries, land areas potentially affected by high flood or debris flow intensities (calculated on the basis of flow heights and/or
 flow velocities), are typically considered as high hazard zones even for low probability events (GAPHAZ, 2017). In Nyalam,
 lower flow heights associated with an outburst from Jialongco result in marginally lower levels of exposure compared to
 430 simulated events from Galongco or the potential future lake (Fig. 6). Despite the majority of buildings in Nyalam being located
 10 – 20 metres above the river channel, where they have been unaffected by past outburst events from Jialongco (Chen *et al.*
 2013), there is clearly significant exposure within the high intensity zone of a worst-case outburst. Furthermore, the rapid
 expansion of infrastructure along the river banks north of the main settlement over the past several years has significantly
 increased the built area exposed to potential GLOF events, with many new buildings located in the high intensity flood zone.
 435 Overall, levels of exposure are comparable for simulated outbursts from both Galongco and the potential future lake, with both
 worst-case events also likely to disrupt the main highway and bridges linking to the town.

Downstream from Nyalam in the reach to the border with Nepal there are few buildings located along the river bank, and the main threat is to the 38 km stretch of the transnational highway, of which the proportion affected by high-intensity flood levels is 27% and 40%, for modelled outbursts from Jialongco and Galongco respectively (and 28% for the future lake scenario). While we did not simulate beyond the border, previous events (e.g., Cook *et al.*, 2018; Wang *et al.*, 2018), and assessment studies (Khanal *et al.*, 2015a; Shrestha *et al.*, 2010) have highlighted the significant risk to Nepalese communities, hydropower stations, and other infrastructure located along the banks of the Bhotekoshi river.



445

Figure 2: A) Built area in Nyalam exposed to modelled GLOF intensity levels for the three assessed lakes, showing the effect of rapid infrastructural development between 2015 and 2017. The percentage indicates the increase in built area within the high intensity zone. B) Modelled intensities for the Galongco outburst scenario showing the recent expansion of infrastructure, as seen in Google

Earth imagery (C) from June 2015 (left) and October 2017 (right). A notable area of infrastructure development just upstream of the main bridge is highlighted in the dashed rectangle.

4.4 Trajectory of future lake development

The thinning of glacier RGI60-15.09475 over at least the last four decades has caused the development of a glacier surface that is well suited for supraglacial lake development (Fig. 7). The central 2.5 km of the glacier's ablation zone, where supraglacial ponds are already forming, is effectively stagnant, very gently sloping and has become heavily pitted due to differential ablation in response to spatially variable debris thickness. These conditions will enable the further expansion of the supraglacial pond network, which is unlikely to drain quickly.

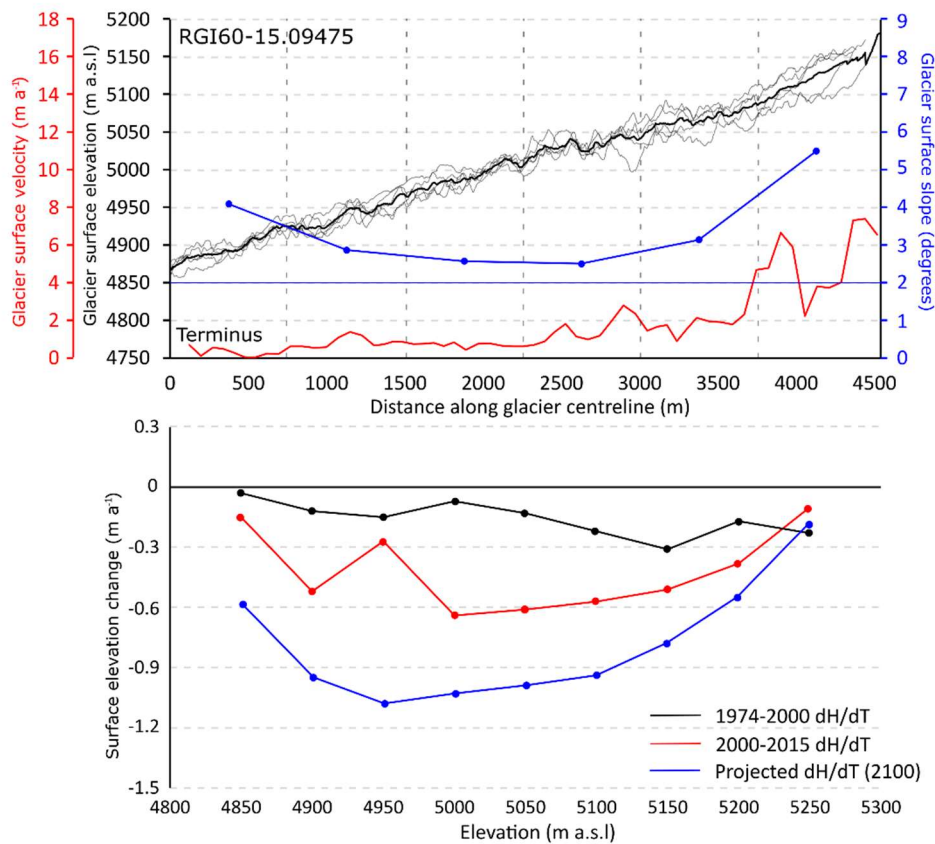


Figure 7: (A) Surface topography, slope, and velocity regime of glacier RGI60-15.09475 in 2017/18. Widespread meltwater ponding is expected once glacier surface slope declines to $\sim 2^\circ$ and little flow is evident to allow for crevasse formation and meltwater drainage. (B) Surface elevation change over the glacier from DEM differencing over the period 1974-2000 and 2000-2015 and the rate of elevation change projected to occur by 2100 (Scenario 1). The same gradient of thinning is assumed to occur by 2056 and be replicated again by 2097 in Scenario 2.

The extrapolation of thinning measured over the last four decades over glacier RGI60-15.09475 suggests that a large portion of the glaciers surface will soon sit below an elevation where supraglacial meltwater would normally drain from the glacier surface, allowing for the development of a supraglacial lake. Under scenario 1 (1974-2015 thinning replicated by 2100), 0.6 km² of the glaciers surface will be below the hydrological base level of the glacier by 2100 (Fig. 8). The majority of this area will be located within 1 km of the glacier's terminal moraine, although some small areas further up-glacier will also sit below the hydrological base level by 2100 due to the glacier's inverse ablation gradient (Fig. 8). Under scenario 2 (1974-2015 thinning

replicated by 2056, 2097), up to 1.33 km² of the surface of glacier RGI60-15.09475 will sit below the hydrological base level of the glacier by 2100. Hence, a large portion of the glacier surface above the 1.54 km² overdeepening identified by GlabTop (Table 3) will have become susceptible to supraglacial lake expansion and proglacial lake formation by 2100 (Fig. 8d). Projected thinning exceeds the ice thickness estimated by GlabTop in current ablation hotspots, most notably towards the terminus of the glacier, where the future ice surface elevation is similar to the simulated bedrock elevation by 2070 under scenario 1 and 2045 under scenario 2. Extrapolated thinning does not match the estimated ice thickness over the majority of the area of the proposed overdeepening further up glacier, where GlabTop suggests ice could be up to 230 m thick.

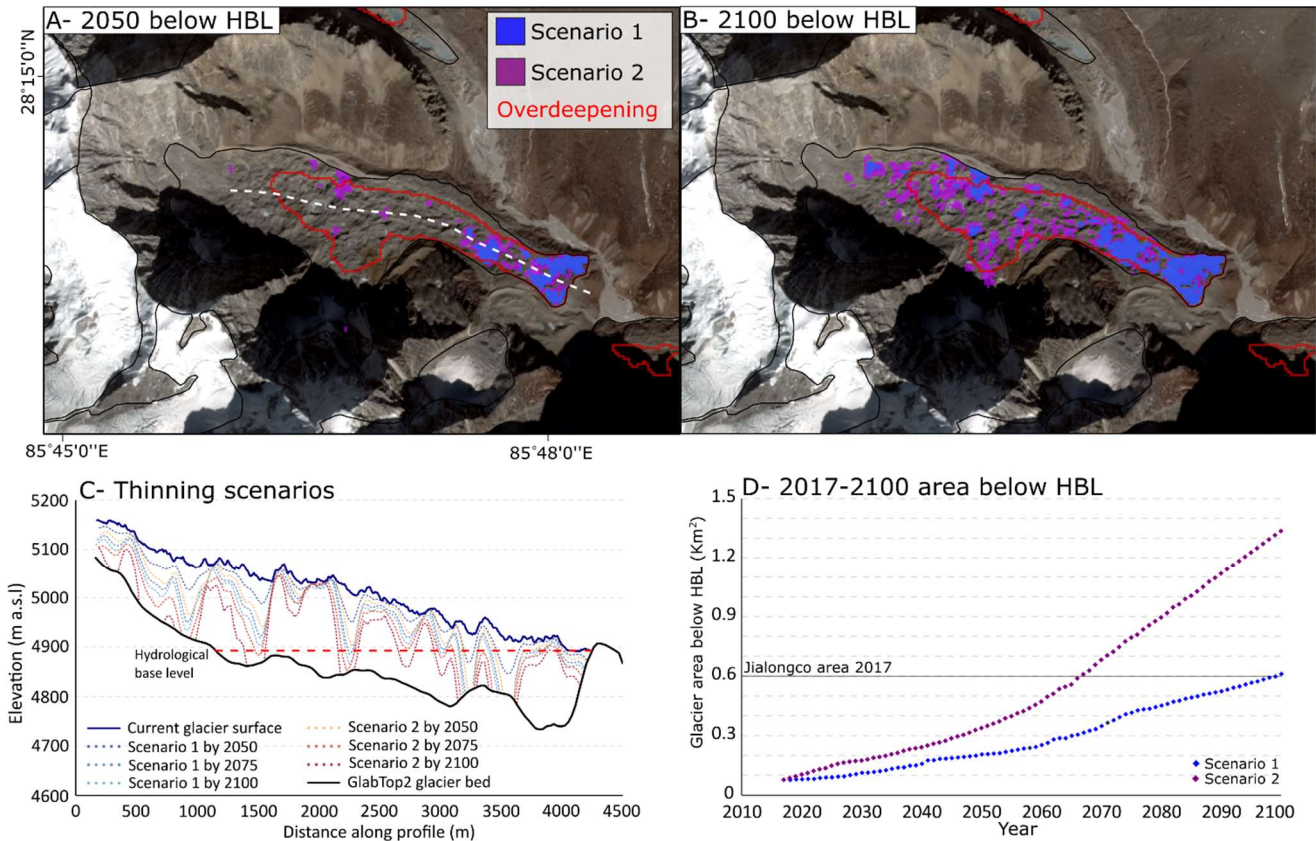


Figure 8: Meltwater ponding (if elevation < the hydrological base level of the glacier) by 2050 (A) and 2100 (B) under different scenarios of thinning for glacier RGI60-15.09475. Glacier surface elevation profiles (taken along profile on panel A) under each scenario of thinning are also shown in panel C. The full timeline of supraglacial lake area expansion is shown in (D). The area within the red polygon shows the location of a bed overdeepening (1.54 km²) predicted by GlabTop. Ice flow is from left to right in A-C.

5 Discussion

The results from this study demonstrate how GLOF hazard assessment at the basin-scale can be expanded to consider new threats that may develop in the future. In doing so, this study has taken established approaches for lake susceptibility assessment (GAPHAZ 2017) and GLOF modelling (Mergili *et al.* 2017) and applied these approaches to consider also an outburst scenario from a potential future lake. To the extent possible, the assessment was based on freely available data and imagery. However, in steep, mountain topography such data can have limitations, and a high-resolution DEM derived from Pleiades imagery was required to achieve accurate GLOF modelling results for Poiqu River basin. While not intended to substitute the comprehensive multi-scenario modeling and field-based hazard mapping that needs to support decision-making (e.g., Frey *et al.*, 2018), the results from this study provide an intermediary step for disaster risk management planning. Using the tools and approaches

demonstrated here, authorities can effectively bridge the knowledge gap between the known threats to which they may already be responding, and those potentially much larger, yet poorly constrained threats that are anticipated to emerge or become more likely in the future.

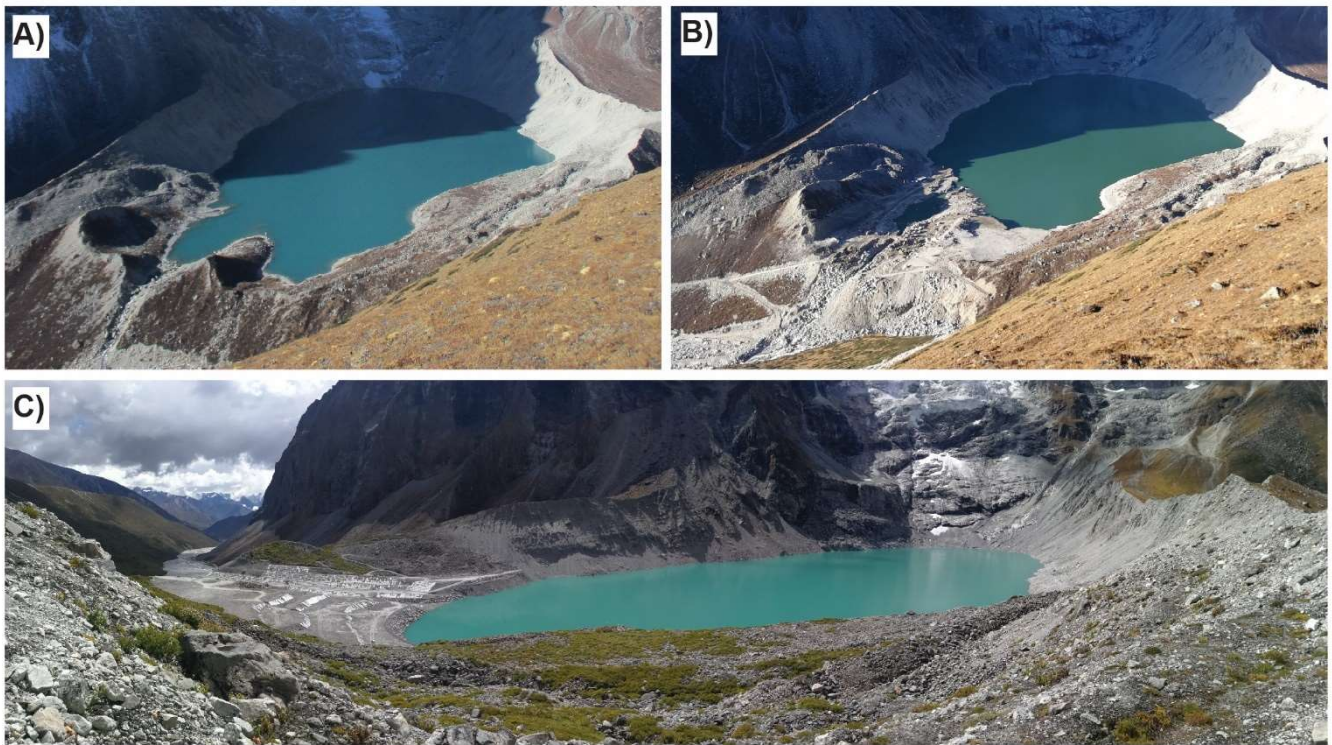
500 For the Poiqu basin, these results come at an opportune time, given that local authorities over the past years have initiated major engineering work at Jialongco (Fig. 9). In principle, the focus of authorities on Jialongco is supported by the results of this study, which indicate that the lake has the greatest likelihood of producing a large GLOF that threatens the village of Nyalam, and, under a worst-case scenario, will lead to significant flood heights and discharges downstream in Nepal. While assessed to be less likely, a large rock/ice-avalanche triggered outburst from Galongco would result in a higher intensity flood event, with discharge values in Nyalam almost 3 times larger than those simulated for Jialongco. At the border with Nepal (Zhangmu), our simulations reveal potential peak discharges in the range of 35,000 – 170,000 m³ s⁻¹ under worst-case scenarios, which is more than 15 times larger than indicated by earlier modelling studies (Shrestha *et al.*, 2010), suggesting that previously estimated potential property losses of up to US\$197 million in downstream communities of Nepal are far lower than what could feasibly occur. In comparison with past events, the 1981 outburst from Cirenmaco, resulting in around 200 fatalities and up to US\$4 million damage, had an estimated peak discharge of around 10,000 m³ s⁻¹ in Zhangmu (Wang *et al.* 2015; Cook *et al.* 2018), while the 2016 event from Gonbatongsha lake was about half this magnitude again, but resulted in economic losses of > US\$ 70 million, but no loss of life (Sattar *et al.* 2022).

Despite the threat the lake poses, the focus at Jialongco on hard engineering strategies to reduce GLOF risk could prove both costly and inefficient, if not complimented by a more comprehensive and forward-looking strategy that considers large process chains and appropriate response actions. The removal and armouring of much of the frontal moraine and construction of a stable outlet channel (Fig. 9) would have only a minimal effect on the potential downstream GLOF magnitudes resulting from a catastrophic ice avalanche into the lake (Figs. 4 and 6). On the one hand, the engineering work has reduced the amount of moraine material available for initial erosion (leading to a more rapid and slowly attenuating water-dominated flow), while on the other hand, the reduction in freeboard has left the lake more susceptible to overtopping, resulting in a larger volume GLOF event (Fig 4a). The simulations also reveal the limited potential for early warning in the case of large process chains, with catastrophic GLOF discharges reaching Nyalam in only 5 – 11 minutes following an ice and/or rock avalanche detaching. For downstream communities in Nepal, warning times under worst-case scenarios could be as little as 30 minutes, which is a significant reduction on current estimates of up to 2 hours in the case of Galongco, whereby a more gradual lake breaching mechanism was modeled (Zhang *et al.* 2021). Particularly in transboundary regions requiring communication and collaboration between countries before any alert is acted upon, minutes lost or gained can be critical for effective early warning and evacuation.

Given the demonstrated minimal effect that lake lowering would have on a potentially devastating, worst-case GLOF from Jialongco, and the fact that warning times for all 3 assessed process chains would be minimal in Nyalam, we argue that a focus on engineering measures and early warning systems needs to be coupled with effective land use zoning and programs to strengthen local response capacities (e.g., Huggel *et al.*, 2020). Such a comprehensive strategy would reduce the risk not only from an outburst from Jialongco, but also provide future-proofing against larger outburst scenarios from Galongco or potential new lakes that develop over the next century. In general, increasing exposure of people and assets is seen as a main driver of disaster risk in mountain regions (Hock *et al.*, 2019), and this is clearly evidenced through the rapid increase in built infrastructure upstream of Nyalam, directly within the high-intensity zone of potential worst-case GLOF events (Fig. 6), but

also within the path of more moderate events (Zhang *et al.* 2021). Lowering of the water level in Jialongco has likely reduced the threat to these buildings from a smaller, higher probability outburst event, but similar action would need to be repeated at Galongco and as new lakes emerge in the future, in order to maintain this minimum level of protection, while doing little to
540 reduce the risk of a larger worst-case event. Land use zoning is therefore urgently required, in order to regulate the future development of infrastructure occurring within high hazard zones, also considering worst-case scenarios. GAPHAZ (2017) draws on the example of Switzerland, where very low probability events are included within a zone of “residual danger” that extends to include events with a return period of up to 300 years. At the least, evacuation centres and other critical infrastructure (e.g. schools, police, medical facilities), should be positioned well out of the potential inundated area. Furthermore, framing
545 any EWS within a broader catchment-scale monitoring program could enable a degree of forecasting, allowing alert levels to be raised and evacuation preparations then initiated within high hazard zones, prior to a warning system being activated. For example, precursory movement associated with recent large high mountain slope failures has been detected with optical or InSAR satellite data (Carla *et al.* 2019; Bhardwaj and Sam 2021), and through dense seismic monitoring networks (Tiwari *et al.* 2022), although real-time operational monitoring systems are rare and should remain an important research priority.

550
While GlabTop and other similar modelling approaches (see Farinotti *et al.*, 2019a) have been widely used to anticipate future glacial lake locations and assess related risks and opportunities (e.g., Farinotti *et al.*, 2019b; Haeberli *et al.*, 2016a; Magnin *et al.*, 2015), large uncertainties remain as to if and when specific overdeepenings will transition into lakes. In this study, we have focussed on a very large overdeepening positioned beneath a flat, heavily debris-covered glacier tongue – a classic
555 geomorphological setting in which large proglacial lakes typically develop (Benn *et al.*, 2012; Haritashya *et al.*, 2018), and analogous to the setting of Galongco. Coupled with the fact that conditions at the surface of the glacier have already allowed supraglacial lakes to form in the ablation zone of the glacier, there can be a high degree of confidence that a future proglacial lake will develop in this location, trapped behind the prominent terminal moraine. Under the two thinning scenarios employed in this study, supraglacial lake area equivalent to the current area of Jialongco will be replicated on glacier RGI60-15.09475
560 by ~2070 to 2100 (Fig. 8). These estimates may still represent a conservatively slower trajectory of lake development on this glacier. Both the development of extensive supraglacial ponds and ice cliff networks and the transition of a supraglacial lake to a full depth proglacial lake can increase the overall thinning rate in the ablation zone of debris-covered glaciers (King *et al.*, 2020; Mölg *et al.*, 2020; Thompson *et al.*, 2016). Our simple extrapolation of current thinning rates and patterns does not account for the initiation or expansion of these ablative processes. Therefore, we would rather expect greater thinning than our
565 results predict in the lowermost ~1.5 km of the glacier over coming decades once a substantial amount of meltwater has ponded at the glaciers surface.



570 **Figure 9: Images taken of Jialongco in A) October 2018 showing the natural state of the lake, B) October 2020 and C) September 2021, showing the engineering work that has been undertaken in the outlet area, lowering the lake level, removing much of the frontal moraine, and establishing a stable, armoured outlet channel. Photos: T. Bolch (A) and G. Zhang (B, C).**

Regardless of uncertainties in the timing of future lake development, the results from this study suggest that hazard mapping and associated response planning that accounts for existing worst-case outburst threats from Jialongco, and particularly Galongco, would largely remain valid for the future lake scenario. In other words, the potential magnitude of a worst-case GLOF from Galongco far exceeds anything the future lake could produce, while a worst-case event from Jialongco has the fastest arrival time in Nyalam. However, the formation of the new lake, and others, will undoubtedly increase the likelihood of a high magnitude event occurring within the basin, and hence, risk levels to people and infrastructure will increase if response strategies are not adequate. One of the key challenges in glacial hazard research is assigning a likelihood or probability to outburst scenarios, particularly for such very large scenarios for which there may be no historical precedence in a given basin (Allen *et al.* 2021). The worst-case scenarios modelled here are an order of magnitude larger than observed or assessed under previous studies (Shrestha *et al.* 2010, Zhang *et al.* 2021), but consider for the first time potential process chains involving large rock/ice avalanches > 20 million m³ striking glacial lakes. The resulting GLOF discharges and flow heights produced by such catastrophic process chains modelled here are certainly extreme, with a return period exceeding 200 years relative to documented discharge values from past GLOFs in Asia (Carrivick *et al.* 2016). However, the recent Chamoli disaster, and earlier events from Seti River, remind that large avalanches capable of triggering such a process chain in the Himalaya do occur (Shugar *et al.* 2021), and their frequency is expected to be increasing as permafrost warms and slopes destabilise (Haeberli *et al.*, 2016b). Combined with larger and more numerous lakes (Zheng *et al.*, 2021b), the likelihood of high-magnitude process chains occurring must be increasing over time, and therefore these more extreme scenarios need to be considered under a comprehensive approach to risk management.

585
590

5 Conclusions

The Poiqu basin in the central Himalaya has been well established as a hotspot from which transboundary GLOF threats can originate. In the current study, we have focused on two lakes that directly threaten the Tibetan town of Nyalam and areas downstream, comparing the likelihood, potential magnitude, and impacts of large outburst events from these lakes. In addition, a future scenario has been modelled, whereby an outburst was simulated for a potential new lake, anticipated to form upstream of Jialongco. For all lakes, worst-case scenarios were assessed, with large rock and/or ice avalanches striking the lakes to trigger GLOF process chains. The study has recognised that:

600

- Jialongco, although smaller in size, poses the most immediate threat to Nyalam and downstream communities, owing to its position beneath a steep, heavily crevassed glacier tongue, and history of outburst events. Even though recent engineering work has lowered the lake level by an average of 16 metres and stabilised the dam area, this has minimal effect on the magnitude and arrival time of a simulated worst-case GLOF triggered by a large ice avalanche.
- The likelihood of a large rock/ice avalanche $>20 \text{ mil m}^3$ striking Galongco is considered very low, but increasing as permafrost slopes warm. The process chain would generate extreme GLOF discharges up to 5 times larger than simulated for Jialongco, resulting in flow heights up to 14 and 17 metres higher in Nyalam and at the border with Nepal (Zhangmu) respectively.
- The assessed future lake could obtain a size comparable to Jialongco by 2070, but possibly earlier as a result of ablative processes around supraglacial ponds and ice cliffs on the debris-covered tongue. Even once the lake obtains its full potential area and volume, a worst-case rock avalanche-triggered outburst will have peak discharges and flow heights that are an order of magnitude lower than what Galongco can produce, but larger than for Jialongco.
- For all three assessed lakes, worst-case outburst events would impact Nyalam within 5-11 minutes of the process chain initiating, while reaching Zhangmu in around 30 minutes, posing severe challenges for early warning and evacuation. While previous studies have focused on rapid lake expansion in the region, for the town of Nyalam, it is rather the expansion of infrastructure directly within the high-intensity flood zone from both current and future lakes that has significantly increased GLOF exposure levels.

610

615

On the basis of these findings, a comprehensive and forward-looking approach to disaster risk reduction is called for, including early warning systems, effective land use zoning and programs to build local response capacities. Relying only on hard engineering strategies at the lake source will prove insufficient, as such strategies do not address underlying exposure and vulnerability to GLOFS and other geohazards, and are demonstrated to be ineffective in the face of worst-case, catastrophic outburst events.

625

Author contribution

SA and AS designed the study and undertook the GLOF modelling, and hazard assessment. OK performed the modelling of future lake development. AB produced the high resolution Pleiades DEM. SA, OK, TB, and GZ provided insights, images and bathymetry data from field visits. All authors contributed to the drafting of the manuscript and funding acquisition.

Acknowledgement

This work was supported by the Swiss National Science Foundation (IZLCZ2_169979/1). The work further benefited from support of the Strategic Priority Research Program of the Chinese Academy of Sciences (XDA20060201). We thank the two anonymous reviewers and Fabian Walter for their extremely comprehensive and constructive comments.

Competing interests

The authors declare that they have no conflict of interest.

640 **References**

- Allen SK, Linsbauer A, Randhawa SS, Huggel C, Rana P, Kumari A. 2016. Glacial lake outburst flood risk in Himachal Pradesh, India: an integrative and anticipatory approach considering current and future threats. *Natural Hazards*. Springer Netherlands **84**(3): 1741–1763. DOI: 10.1007/s11069-016-2511-x.
- 645 Allen SK, Zhang G, Wang W, Yao T, Bolch T. 2019. Potentially dangerous glacial lakes across the Tibetan Plateau revealed using a large-scale automated assessment approach. *Science Bulletin*. Elsevier B.V. **64**(7): 435–445. DOI: 10.1016/j.scib.2019.03.011.
- Allen, SK, Frey, H, Haeberli, W, Huggel, C, Chiarle, M, Geertsema, M. 2022. Assessment Principles for Glacier and Permafrost Hazards in Mountain Regions. *Oxford Research Encyclopedias: Natural Hazard Science*. <https://doi.org/10.1093/acrefore/9780199389407.013.356>
- 650 Benn DI, Bolch T, Hands K, Gulley J, Luckman A, Nicholson LI, Quincey D, Thompson S, Toumi R, Wiseman S. 2012. Response of debris-covered glaciers in the Mount Everest region to recent warming, and implications for outburst flood hazards. *Earth Science Reviews* **114**: 156–174.
- Bhardwaj, A and Sam, L. 2022. Reconstruction and Characterisation of Past and the Most Recent Slope Failure Events at the 2021 Rock-Ice Avalanche Site in Chamoli, Indian Himalaya. *Remote Sensing*, **14** (4), 949, <https://doi.org/10.3390/rs14040949>
- 655 Bhattacharya A, Bolch T, Mukherjee K, King O, Menounos B, Kapitsa V, Neckel N, Yang W, Yao T. 2021. High Mountain Asian glacier response to climate revealed by multi-temporal satellite observations since the 1960s. *Nature Communications* in review.
- Bolch T, Shea JM, Liu S, Azam FM, Gao Y, Gruber S, Immerzeel WW, Kulkarni A, Li H, Tahir AA, Zhang G, Zhang Y. 2019. Status and Change of the Cryosphere in the Extended Hindu Kush Himalaya Region. In: P. W, A. M, A. M and A. S (eds) *The Hindu Kush Himalaya Assessment*. Springer International Publishing: Cham, 209–255. DOI: 10.1007/978-3-319-92288-1_7.
- 660 Bolch T, Yao T, Bhattacharya A, Hu Y, King O, Liu L, Pronk JB, Rastner P, Zhang G. 2002. Earth Observation to Investigate Occurrence, Characteristics and Changes of Glaciers, Glacial Lakes and Rock Glaciers in the Poiqu River Basin (Central Himalaya). *Remote Sensing*, **14**(8):1927, <https://doi.org/10.3390/rs14081927>
- 665 Carlà, T, Intrieri, E, Raspini, F, Bardi, F, Farina, P, Ferretti, A, Colombo, D, Novali, F, Casagli, N. 2019. Perspectives on the prediction of catastrophic slope failures from satellite InSAR. *Scientific Reports*, **9** (1), 14137. <https://doi.org/10.1038/s41598-019-50792-y>.
- Carrivick JL, Tweed FS. 2016. A global assessment of the societal impacts of glacier outburst floods. *Global and Planetary Change*. Elsevier B.V. **144**: 1–16. DOI: 10.1016/j.gloplacha.2016.07.001.
- 670 Chen NS, Hu GS, Deng W, Khanal N, Zhu YH, Han D. 2013. On the water hazards in the trans-boundary Kosi River basin. *Natural Hazards and Earth System Science* **13**(3): 795–808. DOI: 10.5194/nhess-13-795-2013.
- Clague JJ, Evans SG. 2000. A review of catastrophic drainage of moraine-dammed lakes in British Columbia. *Quaternary Science Reviews* **19**: 1763–1783.
- 675 Cook KL, Andermann C, Gimbert F, Adhikari BR, Hovius N. 2018. Glacial lake outburst floods as drivers of fluvial erosion in the Himalaya. *Science (New York, N.Y.)*. American Association for the Advancement of Science **362**(6410): 53–57. DOI: 10.1126/science.aat4981.
- Cook SJ, Quincey DJ. 2015. Estimating the volume of Alpine glacial lakes. *Earth Surface Dynamics* **3**(4): 559–575. DOI: 10.5194/esurf-3-559-2015.
- 680 Emmer A, Cochachin A. 2013. The causes and mechanisms of moraine-dammed lake failures in the Cordillera Blanca,

North American Cordillera, and Himalayas. *AUC Geographica* **48**: 5–15.

Emmer A, Harrison S, Mergili M, Allen S, Frey H, Huggel C. 2020. 70 years of lake evolution and glacial lake outburst floods in the Cordillera Blanca (Peru) and implications for the future. *Geomorphology*. Elsevier B.V. **365**: 107178. DOI: 10.1016/j.geomorph.2020.107178.

685 Farinotti D, Huss M, Fürst JJ, Landmann J, Machguth H, Maussion F, Pandit A. 2019a. A consensus estimate for the ice thickness distribution of all glaciers on Earth. *Nature Geoscience*. Nature Publishing Group **12**(3): 168–173. DOI: 10.1038/s41561-019-0300-3.

Farinotti D, Round V, Huss M, Compagno L, Zekollari H. 2019b. Large hydropower and water-storage potential in future glacier-free basins. *Nature*. Springer US **575**(7782): 341–344. DOI: 10.1038/s41586-019-1740-z.

690 Frey H, Huggel C, Chisolm RE, Baer P, Mcardell BW, Cochachin A, Portocarrero. 2018. Multi-source glacial lake outburst flood hazard assessment and mapping for Huaraz, Cordillera Blanca, Peru. . DOI: 10.3389/feart.2018.00210.

Frey H, Haeberli W, Linsbauer A, Huggel C, Paul F. 2010. A multi-level strategy for anticipating future glacier lake formation and associated hazard potentials. *Natural Hazards and Earth System Sciences* **10**: 339–352.

695 Fujita K, Sakai A, Takenaka S, Nuimura T, Surazakov AB, Sawagaki T, Yamanokuchi T. 2013. Potential flood volume of Himalayan glacial lakes. *Natural Hazards and Earth System Science* **13**(7): 1827–1839. DOI: 10.5194/nhess-13-1827-2013.

Furian W, Loibl D, Schneider C. 2021. Future glacial lakes in High Mountain Asia: an inventory and assessment of hazard potential from surrounding slopes. *Journal of Glaciology*. Cambridge University Press (CUP) 1–18. DOI: 10.1017/jog.2021.18.

700 GAPHAZ. 2017. *Assessment of Glacier and Permafrost Hazards in Mountain Regions: Technical Guidance Document*. Standing Group on Glacier and Permafrost Hazards in Mountains (GAPHAZ) of the International Association of Cryospheric Sciences (IACS) and the International Permafrost Association (IPA). Zurich, Switzerland / Lima, Peru.

705 Gardelle J, Arnaud Y, Berthier E. 2011. Contrasted evolution of glacial lakes along the Hindu Kush Himalaya mountain range between 1990 and 2009. *Global and Planetary Change* **75**: 47–55.

Haeberli W, Buetler M, Huggel C, Lehmann Friedli T, Schaub Y, Schleiss AJ. 2016a. New lakes in deglaciating high-mountain regions – opportunities and risks. *Climatic Change* **139**: 201–214.

710 Haeberli W, Schaub Y, Huggel C. 2016b. Increasing risks related to landslides from degrading permafrost into new lakes in de-glaciating mountain ranges. *Geomorphology* doi: 10.1016/j.geomorph.2016.02.009.

Haritashya UK, Kargel JS, Shugar DH, Leonard GJ, Strattman K, Watson CS, Shean D, Harrison S, Mandli KT, Regmi D. 2018. Evolution and controls of large glacial lakes in the Nepal Himalaya. *Remote Sensing* **10**(5): 1–31. DOI: 10.3390/rs10050798.

715 Hock R, Rasul G, Adler C, Cáceres B, Gruber S, Hirabayashi Y, Jackson M, Kääb A, Kang S, Kutuzov S, Milner A, Molau U, Morin S, Orlove B, Steltzer H. 2019. *High Mountain Areas*. In: *IPCC Special Report on the Ocean and Cryosphere in a Changing Climate* [H.-O. Pörtner, D.C. Roberts, V. Masson-Delmotte, P. Zhai, M. Tignor, E. Poloczanska, K. Mintenbeck, A. Alegria, M. Nicolai, A. Okem, J. Petzold, B. Rama, N.M. .

Huggel C, Cochachin A, Drenkhan F, Fluixá-Sanmartín J, Frey H, García Hernández J, Jurt C, Muñoz R, Price K, Vicuña L. 2020. Glacier Lake 513, Peru: lessons for early warning service development. *WMO Bulletin* **69**(1): 45–52.

720 Huggel C, Haeberli W, Kääb A, Bieri D, Richardson S. 2004. An assessment procedure for glacial hazards in the Swiss

Alps. *Canadian Geotechnical Journal* **41**: 1068–1083.

- 725 Kääh A, Jacquemart M, Gilbert A, Leinss S, Girod L, Huggel C, Falaschi D, Ugalde F, Petrakov D, Chernomorets S, Dokukin M, Paul F, Gascoin S, Berthier E, Kargel JS. 2021. Sudden large-volume detachments of low-angle mountain glaciers – more frequent than thought? *The Cryosphere* **15**(4): 1751–1785. DOI: 10.5194/tc-15-1751-2021.
- Khanal NR, Hu J-M, Mool P. 2015a. Glacial Lake Outburst Flood Risk in the Poiqu/Bhote Koshi/Sun Koshi River Basin in the Central Himalayas. *Mountain Research and Development* **35**: 351–364.
- 730 Khanal NR, Mool PK, Shrestha AB, Rasul G, Ghimire PK, Shrestha RB, Joshi SP. 2015b. A comprehensive approach and methods for glacial lake outburst flood risk assessment, with examples from Nepal and the transboundary area. *International Journal of Water Resources Development* **31**: 219–237.
- King O, Bhattacharya A, Bhambri R, Bolch T. 2019. Glacial lakes exacerbate Himalayan glacier mass loss. *Scientific Reports*. Nature Research **9**(1). DOI: 10.1038/s41598-019-53733-x.
- 735 King O, Bhattacharya A, Ghuffar S, Tait A, Guilford S, Elmore AC, Bolch T. 2020. Six Decades of Glacier Mass Changes around Mt. Everest Are Revealed by Historical and Contemporary Images. *One Earth*. Cell Press **3**(5): 608–620. DOI: 10.1016/j.oneear.2020.10.019.
- King O, Dehecq A, Quincey D, Carrivick J. 2018. Contrasting geometric and dynamic evolution of lake and land-terminating glaciers in the central Himalaya. *Global and Planetary Change*. Elsevier B.V. **167**: 46–60. DOI: 10.1016/j.gloplacha.2018.05.006.
- 740 Korup O, Tweed F. 2007. Ice, moraine, and landslide dams in mountainous terrain. *Quaternary Science Reviews* **26**: 3406–3422.
- Kraaijenbrink PDA, Bierkens MFP, Lutz AF, Immerzeel WW. 2017. Impact of a global temperature rise of 1.5 degrees Celsius on Asia’s glaciers. *Nature Publishing Group* **549**: 5–7. DOI: 10.1038/nature23878.
- 745 Linsbauer A, Frey H, Haeberli W, Machguth H, Azam MF, Allen S. 2016. Modelling glacier-bed overdeepenings and possible future lakes for the glaciers in the Himalaya–Karakoram region. *Annals of Glaciology* **57**: 119–130.
- Linsbauer A, Paul F, Haeberli W. 2012. Modeling glacier thickness distribution and bed topography over entire mountain ranges with GlabTop: application of a fast and robust approach. *Journal of Geophysical Research* **117**: doi: 10.1029/2011JF002313.
- 750 Linsbauer A, Paul F, Machguth H, Haeberli W. 2013. Comparing three different methods to model scenarios of future glacier change in the Swiss Alps. *Annals of Glaciology* **54**: 241–253.
- Liu J-J, Tang C, Cheng Z-L. 2013. The Two Main Mechanisms of Glacier Lake Outburst Flood in Tibet, China. *J. Mt . Sci* **10**(2): 239–248. DOI: 10.1007/s11629-013-2517-8.
- 755 Lliboutry L, Morales AB, Pautre A, Schneider B. 1977. Glaciological problems set by the control of dangerous lakes in Cordillera Blanca, Peru. I. Historic failure of morainic dams, their causes and prevention. *Journal of Glaciology* **18**: 239–254.
- Magnin F, Haeberli W, Linsbauer A, Deline P, Ravel L. 2020. Estimating glacier-bed overdeepenings as possible sites of future lakes in the de-glaciating Mont Blanc massif (Western European Alps). *Geomorphology*. Elsevier B.V. **350**. DOI: 10.1016/j.geomorph.2019.106913.
- 760 Magnin F, Krautblatter M, Deline P, Ravel L, Malet E, Bevington A. 2015. Determination of warm, sensitive permafrost areas in near-vertical rockwalls and evaluation of distributed models by electrical resistivity tomography. *Journal of Geophysical Research-Earth Surface* **120**: 745–762.
- Maurer JM, Schaefer JM, Rupper S, Corley A. 2019. Acceleration of ice loss across the Himalayas over the past 40

- years. *Science Advances*. American Association for the Advancement of Science **5**(6): eaav7266. DOI: 10.1126/sciadv.aav7266.
- 765 Mölg N, Ferguson J, Bolch T, Vieli A. 2020. On the influence of debris cover on glacier morphology: How high-relief structures evolve from smooth surfaces. *Geomorphology*. Elsevier B.V. **357**: 107092. DOI: 10.1016/j.geomorph.2020.107092.
- Nie Y, Liu Q, Wang J, Zhang Y, Sheng Y, Liu S. 2018. An inventory of historical glacial lake outburst floods in the Himalayas based on remote sensing observations and geomorphological analysis. *Geomorphology*. Elsevier B.V. **308**: 91–106. DOI: 10.1016/j.geomorph.2018.02.002.
- 770 Nie Y, Sheng Y, Liu Q, Liu L, Liu S, Zhang Y, Song C. 2017. A regional-scale assessment of Himalayan glacial lake changes using satellite observations from 1990 to 2015. *Remote Sensing of Environment*. Elsevier Inc. **189**: 1–13. DOI: 10.1016/j.rse.2016.11.008.
- Pronk JB, Bolch T, King O, Wouters B, Benn DI. 2021. Proglacial Lakes Elevate Glacier Surface Velocities in the Himalayan Region. *The Cryosphere Discussions* in review. DOI: 10.5194/tc-2021-90.
- 775 Quincey DJ, Richardson SD, Luckman A, Lucas RM, Reynolds JM, Hambrey MJ, Glasser NF. 2007. Early recognition of glacial lake hazards in the Himalaya using remote sensing datasets. *Global and Planetary Change* **56**: 137–152.
- Ren Y-Y, Ren G-Y, Sun X-B, Shrestha AB, You Q-L, Zhan Y-J, Rajbhandari R, Zhang P-F, Wen K-M. 2017. Observed changes in surface air temperature and precipitation in the Hindu Kush Himalayan region over the last 100-plus years. *Advances in Climate Change Research* **8**(3): 148–156. DOI: 10.1016/j.accre.2017.08.001.
- 780 Richardson SD, Reynolds JM. 2000. An overview of glacial hazards in the Himalayas. *Quaternary International* **65/66**: 31–47.
- Sanjay J, Krishnan R, Shrestha AB, Rajbhandari R, Ren GY. 2017. Downscaled climate change projections for the Hindu Kush Himalayan region using CORDEX South Asia regional climate models. *Advances in Climate Change Research*. National Climate Center **8**(3): 185–198. DOI: 10.1016/j.accre.2017.08.003.
- 785 Sattar A, Haritashya UK, Kargel JS, Leonard GJ, Shugar DH, Chase D V. 2021. Modeling Lake Outburst and Downstream Hazard Assessment of the Lower Barun Glacial Lake, Nepal Himalaya. *Journal of Hydrology*. Elsevier BV **598**: 126208. DOI: 10.1016/j.jhydrol.2021.126208.
- 790 Schmid M-O, Baral P, Gruber S, Shahi S, Shrestha T, Stumm D, Wester P. 2015. Assessment of permafrost distribution maps in the Hindu Kush Himalayan region using rock glaciers mapped in Google Earth. *The Cryosphere* **9**: 2089–2099.
- Schneider D, Huggel C, Haeberli W, Kaitna R. 2011. Unraveling driving factors for large rock-ice avalanche mobility. *Earth Surface Processes and Landforms* **36**: 1948–1966.
- 795 Shedlock KM, Giardini D, Grünthal G, Zhang P. 2000. The GSHAP Global Seismic Hazard Map. *Seismological Research Letters*. Seismological Society of America **71**(6): 679–686. DOI: 10.1785/gssrl.71.6.679.
- Shijin W, Shitai J. 2015. Evolution and outburst risk analysis of moraine-dammed lakes in the central Chinese Himalaya. *Journal of Earth System Science*. Springer India **124**(3): 567–576. DOI: 10.1007/s12040-015-0559-8.
- 800 Shrestha AB, Eriksson M, Mool P, Ghimire P, Mishra B, Khanal NR. 2010. Glacial lake outburst flood risk assessment of Sun Koshi basin, Nepal. *Geomatics, Natural Hazards and Risk*. Taylor & Francis **1**(2): 157–169. DOI: 10.1080/19475701003668968.
- Shugar DH, Burr A, Haritashya UK, Kargel JS, Watson CS, Kennedy MC, Bevington AR, Betts RA, Harrison S,

- 805 Strattman K. 2020. Rapid worldwide growth of glacial lakes since 1990. *Nature Climate Change*. Springer US
10(10): 939–945. DOI: 10.1038/s41558-020-0855-4.
- Thompson S, Benn DI, Mertes J, Luckman A. 2016. Stagnation and mass loss on a Himalayan debris-covered glacier:
Processes, patterns and rates. *Journal of Glaciology*. International Glaciology Society **62**(233): 467–485. DOI:
10.1017/jog.2016.37.
- 810 Tiwari, A, Sain, K, Kumar, A, Tiwari, J, Paul, A, Kumar, N, Haldar, C, Kumar, S, Pandey, CP. 2022. Potential seismic
precursors and surficial dynamics of a deadly Himalayan disaster: an early warning approach. *Scientific
Reports*, **12**(1), 3733. <https://doi.org/10.1038/s41598-022-07491-y>
- Veh G, Korup O, von Specht S, Roessner S, Walz A. 2019. Unchanged frequency of moraine-dammed glacial lake
outburst floods in the Himalaya. *Nature Climate Change*. Nature Publishing Group, 379–383. DOI:
10.1038/s41558-019-0437-5.
- 815 Wang S, Dahe Q, Xiao C. 2015a. Moraine-dammed lake distribution and outburst flood risk in the Chinese Himalaya.
Journal of Glaciology **61**: 115–126.
- Wang S, Zhou L. 2017. Glacial Lake Outburst Flood Disasters and Integrated Risk Management in China. *International
Journal of Disaster Risk Science* **8**. DOI: 10.1007/s13753-017-0152-7.
- 820 Wang W, Gao Y, Iribarren Anacona P, Lei Y, Xiang Y, Zhang G, Li S, Lu A. 2018. Integrated hazard assessment of
Cirenmaco glacial lake in Zhangzangbo valley, Central Himalayas. *Geomorphology*
<http://dx.doi.org/10.1016/j.geomorph.2015.08.013>.
- Wang W, Xiang Y, Gao Y, Lu A, Yao T. 2015b. Rapid expansion of glacial lakes caused by climate and glacier retreat
in the Central Himalayas. *Hydrological Processes*. John Wiley & Sons, Ltd **29**(6): 859–874. DOI:
10.1002/hyp.10199.
- 825 Westoby MJ, Glasser NF, Brasington J, Hambrey MJ, Quincey DJ, Reynolds JM. 2014. Modelling outburst floods from
moraine-dammed glacial lakes. *Earth-Science Reviews* **134**: 137–159. DOI:
<http://dx.doi.org/10.1016/j.earscirev.2014.03.009>.
- Worni R, Stoffel M, Huggel C, Volz C, Casteller A, Luckman B. 2012. Analysis and dynamic modeling of a moraine
failure and glacier lake outburst flood at Ventisquero Negro, Patagonian Andes (Argentina). *Journal of*
830 *Hydrology* **444–445**: 134–145.
- Zemp M, Huss M, Thibert E, Eckert N, McNabb R, Huber J, Barandun M, Machguth H, Nussbaumer SU, Gärtner-Roer
I, Thomson L, Paul F, Maussion F, Kutuzov S, Cogley JG. 2019. Global glacier mass changes and their
contributions to sea-level rise from 1961 to 2016. *Nature*. Nature Publishing Group, 382–386. DOI:
10.1038/s41586-019-1071-0.
- 835 Zhang G, Bolch T, Allen S, Linsbauer A, Chen W, Wang W. 2019. Glacial lake evolution and glacier–lake interactions
in the Poiqu River basin, central Himalaya, 1964–2017. *Journal of Glaciology*. Cambridge University Press
1–19. DOI: 10.1017/jog.2019.13.
- Zhang G, Yao T, Xie H, Wang W, Yang W. 2015. An inventory of glacial lakes in the Third Pole region and their
changes in response to global warming. *Global and Planetary Change* **131**: 148–157.
- 840 Zhang, T, Wang, W, Gao, T. An, B. 2021. Simulation and Assessment of Future Glacial Lake Outburst Floods in the
Poiqu River Basin, Central Himalayas. *Water*, **13**(1376), <https://doi.org/10.3390/w13101376>.
- Zheng G, Allen SK, Bao A, Ballesteros-Cánovas JA, Huss M, Zhang G, Li L, Yuan Y, Jiang L, Yu T, Chen W, Stoffel
M. 2021a. Increasing risk of glacial lake outburst floods from future Third Pole deglaciation. *Nature Climate
Change* <https://doi.org/10.1038/s41558-021-01028-3>.

845 Zheng G, Mergili M, Emmer A, Allen S, Bao A, Guo H, Stoffel M. 2021b. The 2020 glacial lake outburst flood at Jinwuco, Tibet: causes, impacts, and implications for hazard and risk assessment. *The Cryosphere Discussions* 1–28. DOI: 10.5194/tc-2020-379.